MODELING AND MANUFACTURING OF MINIATURE COILS FOR Ni-Mn-Ga MICRO-DEVICES

Lappeenranta-Lahti University of Technology LUT

Master's Program in Computational Engineering, Master's Thesis

2022

Eleonora Raldugina

Examiner: Professor Kari Ullakko
D.Sc. (Tech.) Ville Laitinen

ABSTRACT

Lappeenranta-Lahti University of Technology LUT
School of Engineering Science
Computational Engineering

Eleonora Raldugina

Modeling and manufacturing of miniature coils for Ni-Mn-Ga micro-devices

Master's thesis
2022
47 pages, 44 figures, 6 tables, 0 appendices
Examiners: Professor Kari Ullakko and D.Sc. (Tech.) Ville Laitinen

Keywords: MSM, MSM devices, Magnetic shape memory devices, NiMnGa actuators

This thesis is aimed to develop a miniature copper coil for use in Ni-Mn-Ga-based magnetic shape memory alloy micro-devices. The research focus is mainly on the copper coil geometry calculation. The used calculation model is based on the finite element method (FEM). The calculations are performed to find the effect of the main parameters of copper coil geometry and to find the optimal parameters values to create the required magnetic field strength. The presented calculations are confirmed by experimental results. Additionally, it was shown that copper coils can be successfully produced via femtosecond pulsed laser micromachining and the performed calculations are validated via measurements conducted on the manufactured coils.

ACKNOWLEDGEMENTS

I would like to thank my supervisors Professor Kari Ullakko and Dr. Ville Laitinen. I would like also to thank Aditya Kumthekar and Egor Fadeev for help in experimental sample production and Dr. Andrey Saren for guidance in experimental measurements.

Lappeenranta, April 22, 2022

Eleonora Raldugina

LIST OF ABBREVIATIONS

MSM	Magnetic shape memory
FEM	Finite element method
A	Ampere
V	Volts
T	Tesla
PCB	Printed circuit board
DXF	Short for Drawing Exchange Format. Data file format developed by Autodesk

CONTENTS

1 INTRODUCTION

1.1 Background

In this master thesis it is required to create a coil. According to the definition, coil is an element of electric circuit. Usually, this element has round or round-like shape and may have one or many turns (Fig. 1) [1]. Coils are usually used to create a magnetic field or to provide specific electrical resistance.

Usually, coils are used to create high inductance while its resistance and capacity remain low. These components are usually used in power electronics for voltage levels transformation. Another quite popular application for coils are different oscillatory circuits. As it can be seen from the given examples, the coil size is a second question for such applications. The only parameter that may constrain the coils size is the size of the PCB (printed circuit board) (or ready device), if the coil is implemented in such a system. The main parameters for such coils are their inductance, resistance and capacity. For coils that are used in power electronics, it is also important to have a device where coil can work with high voltages and currents. Such coil applications have limitation concerning the minimum width of the applicable conductors. Fig. 1 represents two typical coil geometries.

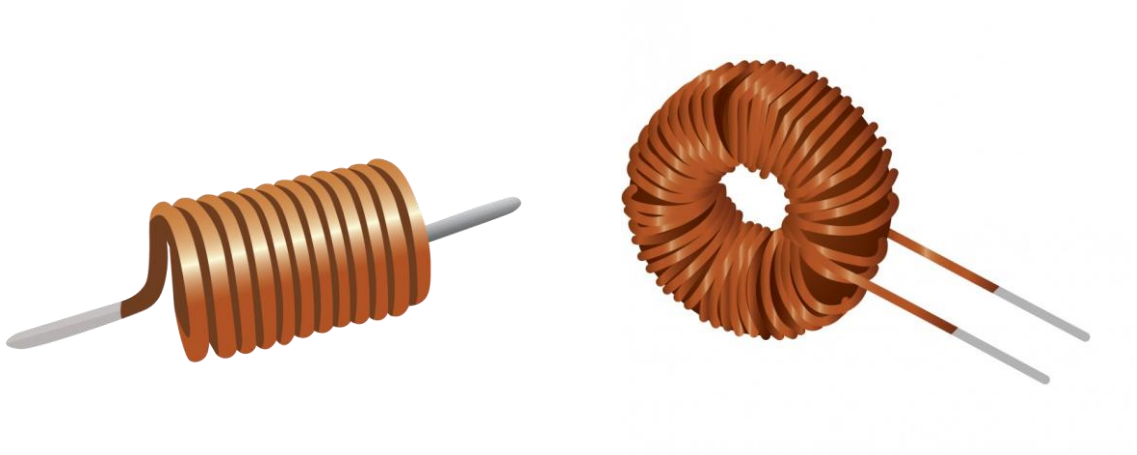

(a) (b)

Figure 1. Images of typical coil geometries [2]

As it can be seen from Fig. 1, typical ‘general purpose’ coil has several turns that are placed one over the other. Another type of geometry is so-called ‘tor’ (Fig. 1.b) that is quite popular in transformers and solenoids. This geometry is similar to the plain vertical coil. The only difference is that the lowest and the highest turns are brought to each other. Both discussed geometries allow to increase the magnetic field created by the coil turns. Usually, the inductors with such geometry types are additionally wrapped around some magnetic material that increases coil inductance even more. For these purposes, coils usually are produced as ready-to-use components. It is important to ensure that the coil turns are fixed in space and do not go loose during the device work and transportation, which can create a challenge for the coil manufacturers and distributors.

However, there are some specific applications that demand copper coils to have different shapes. For example, in this work, it is required to design a flat one-dimensional coil (see section 1.2), which is different from the typical geometries discussed earlier. The main difference for the designed coil geometry is that the height and overall coil size need to be scaled down to miniaturized sizes required by the target application. Such demands for previous applications were irrelevant, asthe final designed device size where the coil was used was significantly bigger than the inductor itself. The coil that was designed in this master thesis uses the circular spiral as the coil geometry. The basic assumption is that the number of turns in resulting spiral of new geometry is equivalent to the number of turns in regular geometry (compare to Fig. 1).

This geometry allows one to obtain the same effect from the coils with fewer turns of the conductor placed one over the other in one dimension. Coil turns that were placed above the previous one in the conventional geometries are placed around the "lowest" coil turn in the designed geometry. This geometry is much easier to produce, as the production process does not require any additional manufacturing equipment, such as coil winding machines, for example. Instead, this geometry can be produced directly from copper foil using pulsed laser micromachining. This type of coil also makes designed this way inductor highly scalable, which is vital for this coil target application.

It is also worth mentioning that this coil is designed to conduct short powerful current pulses. And it is possible that number of the designed coil geometry applications will significantly grow from specific devices that are discussed in section 1.2 to more generic ones. Nevertheless, weak sides of this geometry, such as small areas, where the required magnetic field will be created, the necessity to have quite large and short current pulses and some limitations for the number of turns in such spirals (section 4.1) make the use of such geometryin regular (for generic inductor applications) coil scale very unrealistic.

1.2 Target application

This work is devoted to the development of the copper coil. The main purpose of this coil is to create large enough magnetic field (minimum of approximately 0.5 T) in a small area inside the Ni-Mn-Ga sample. This material is known as a magnetic shape memory (MSM) alloy. MSM alloys are a class of materials that show the presence of the mechanical stress and subsequent large magnetic-field-induced stains of several percent [3, 4] when magnetic field is applied. The material can be brought back to its initial state (from the changed geometry state) by spring force or by applying a magnetic field in 90 degrees angle in comparison to the initial direction of the field [4].

MSM alloys show large potential for practical applications. For example, there is an active development of the medical sensors based on the MSM material [5]. That shows the biological system change through the thin MSM alloy state change. Traditionally, this type of device mostly uses ZnO based materials. Another quite popular practical application of the MSM materials is a smart micro-actuator [6]. These devicesare already applied in autonomous generators [7]. According to the research [7], they can generate ultra-low frequencies of about 0.5 Hz or less. It is worth also mentioning that output signal frequency also depends on the power on which generator is operated. In addition, there exist several studies that investigate the MSM materials as mechanical sensors [8]. The censoring method in this cited study is based on detecting the reorientation of the martensitic variants in the tetragonal unit cell of the atomic lattice of the alloy.

1.3 Objectives and delimitations

The designed system consists of two copper spirals. These spirals create a magnetic field with a magnetic flux density of 1 T or greater. The magnetic field is supposed to be created with current pulses that are longer than 1 microsecond. Ni-Mn-Ga sample is supposed to be placed in the middle of the spirals between two copper coils (Fig. 2). From the material properties, it is known that it is required to calculate the copper coil size, shape, and thickness for creating the field of B = 0.5 T in the given volume. The geometry of this task is presented in the Fig. 2 and Fig. 3. The generated field should be controlled with the rectangular pulses from 1 ms to 1 s long. It is also necessary to calculate the heating of the wire and the plate.

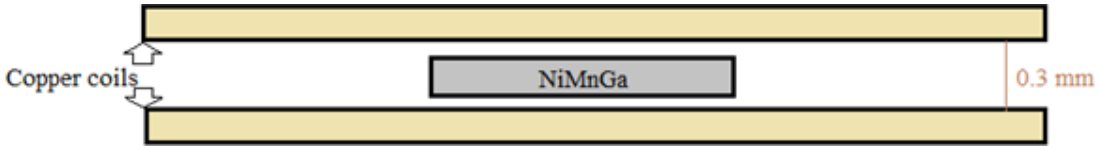

Figure 2. Geometry of the designed system

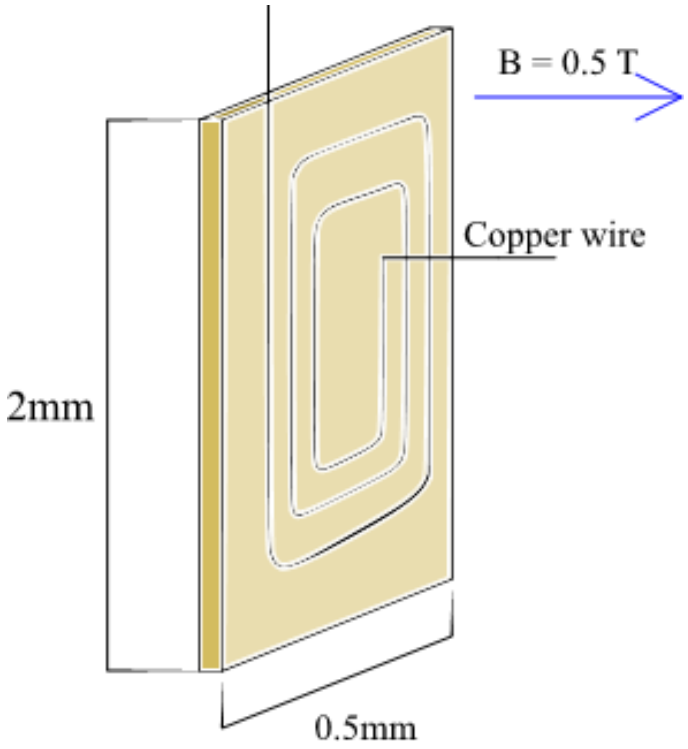

Figure 3. The geometry of the magnetic field calculation problem

1.4 Structure of the thesis

Current study at first sets the task in chapter 1. Then in chapter 2 calculation model is discussed. In this chapter also the geometry of the coil is discussed. These calculations are also used for the experimental part that is described in a chapter 3. This chapter is mostly devoted to the experiment methods and results discussion. This chapter also contains the copper coil geometry modification for femtosecond pulsed laser micromachining process. This chapter also contains the experimental setup description. The next chapter (chapter 4) is devoted to the calculation part of the research. The chapter consists of 4 parts: the first part of it is devoted to the research of the main parameters influence on designed geometry. The second part is devoted to the system scalability research. The third part is about the calculations for copper spiral with complex rectangular geometry. The fourth part is the preliminary calculations for single turn coils that are not limited by the technological limits and can

create large enough field for small scale applications. All the results are aligned in discussion and the work is summarized with results discussion. This chapter contains comparison of the calculated device with numeric characteristics of already existing one.

2 CALCULATION MODEL

Current calculation model is created in software package Comsol multi-physics [9]. This model is based on the Finite Element Method (FEM). This method presents differential equations as the increment ratio of the function value to the difference of its arguments. The achieved set of the equations is suitable for computer-aided calculations.

2.1 Calculation Model and its Description

The described system from chapter 1 is calculated with two models. The first model is a number of several copper rings of different radiuses. This model allows present the spiral as a coil as a number of copper rings. For each ring, the Helmholtz law is applied. As a result, the magnetic field distribution is presented as a superposition of field distributions that were calculated for different rings separately. Model is numerically calculated in program Comsol [9]. Model geometry is presented in the Fig. 4.

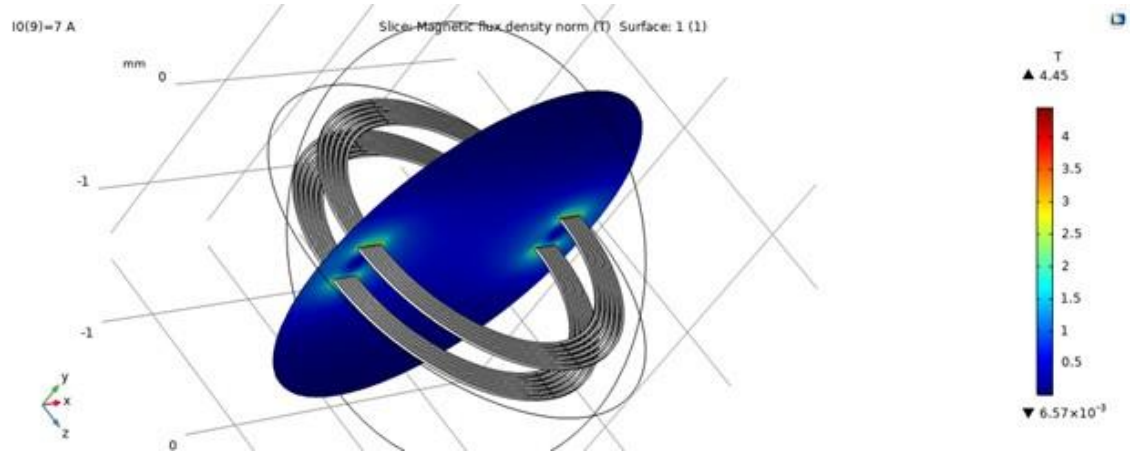

Figure 4. First model geometry representation

The second model calculates the pulse duration. The main purpose of this model is to determine the copper spiral heating. Therefore, this model recreates the exact geometry (Fig. 5).

As it can be seen from the figure above, copper spiral is in shape of Archimedes spiral. This version of spiral has constant distance between the spiral loops. This geometry is the

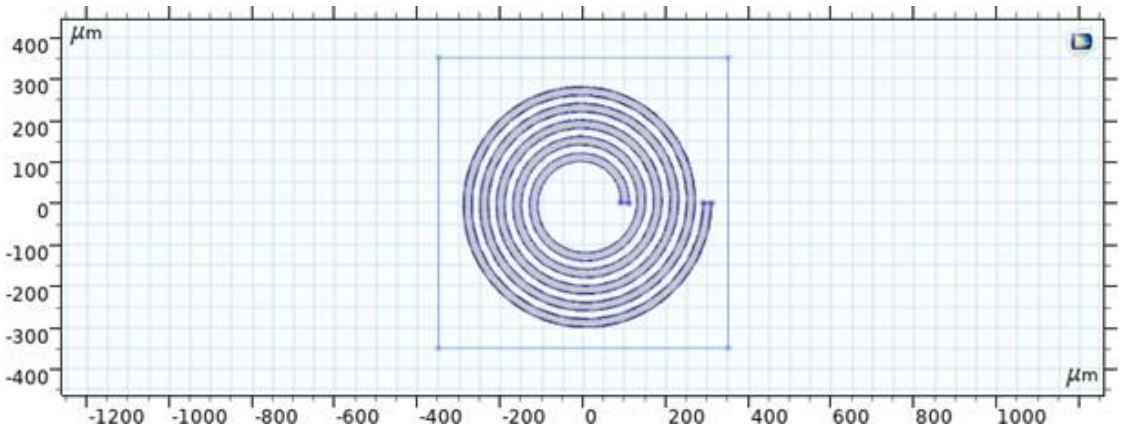

Figure 5. Second model geometry representation

simplest one. Its symmetry makes this system easy to calculate and to manufacture.

2.2 Minimal current calculation

It is required to determine the minimal value of the current for two copper coils. For that purpose, parametric sweep calculation method was used. The value of the current and the flux density B that were received during this study are listed in Table 1.

The coil is presented as a number of five coils for each spiral. The research was conducted for ten different types of current (0.01 A, 0.05 A, 0.1 A, 0.15 A, 0.2 A, 0.3 A, 0.5 A, 0.7 A, 1 A, 2 A). The field maxima (figure 2.1) are placed at the center between two coils.

Table 1. Flux density B dependency on the current I.

Flux density B_{max}, T	Current I, A
$3.75*10^{-3}$	0.01
0.02	0.05
0.04	0.1
0.06	0.15
0.08	0.2
0.11	0.3
0.19	0.5
0.5	0.7
0.38	1
0.44	2

As we can see from above, the minimal current of each coil is equal to 0.3 A. The maximum value of the magnetic flux density for this current is equal to 0.11 T. Therefore, it is possible to create the required magnetic flux density with just two coils simply by increasing the current value.

2.3 Geometry calculation problem set

In previous section the geometry for two spirals geometry was modeled. It is required to pass through the coil current I = 2 A to receive the flux density value above 0.5 T. Then it is required to determine how small the system can be to generate the same flux density value and to endure the heat caused by the current. As the result of the chapter, the geometrical numeric parameters of the system will be given in the first part, and the highest possible pulse length will be given in the second part pf the report. All the modeling will be held based on two models. These two models were described in the previous chapter. This model it is a deviation from the Helmholtz circles problem for given geometry. The magnetic field is calculated not for one spiral but for 5 circle wires, where each circle is a turn of a coil. Its initialgeometry is given in Fig. 6. The second model is used to calculate heating and system scalability of the spiral geometry. This model is less suitable for magneticflux density calculations. However, it is extremely useful for Joule heating calculations due to specific geometry recreation. The geometry of this spiral is given in the Fig. 7.

2.4 System scalability calculations

The first system that is used for scalability is the same one that was created in previous chapter. Fig. 6 shows the initial system setup before the scaling the studied spiral model slice. The slice position matches the symmetry axis.

The main system scalability limitations relate to the production process. The best way to produce the spiral is the photolithography method. Therefore, the main limitations will be connected to this method limitations. Standard gap limitation for contact lithography method is from 20 to 40 μm. Therefore, the minimal value of the gap and spiralthickness is 20 μm. The second possible limitation is the finite value of the electric strength of the material. This limitation can be assessed with the second model (Fig. 7). In this model, a single copper spiral is used. Fig. 7 contains the smallest possible geometry of the coil from the lithography point of view. The third limitation for coil sizeis the magnetic field distribution (Fig. 8). The following figure demonstrates that the area

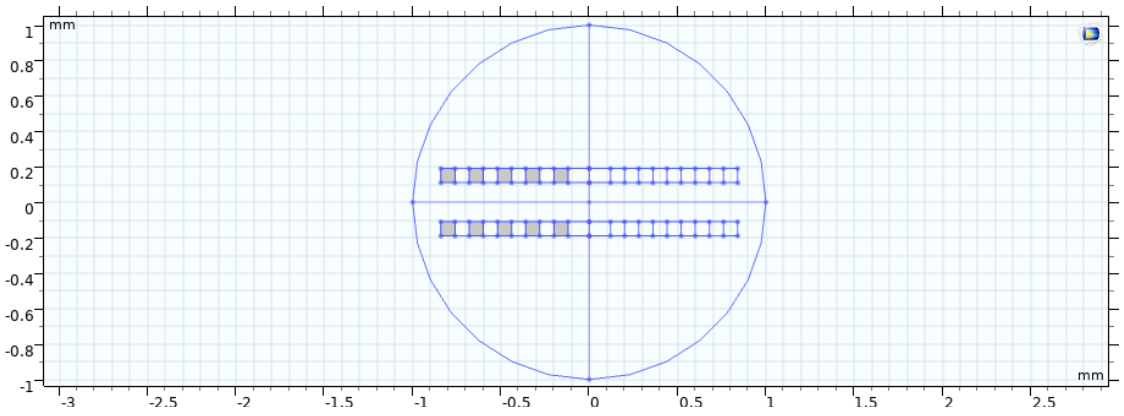

Figure 6. The first spiral model slice

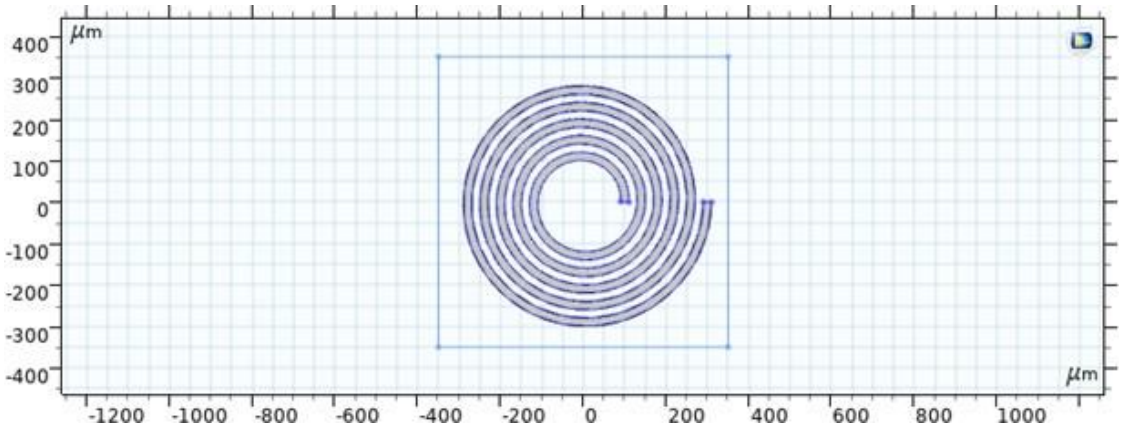

Figure 7. Second copper spiral model for heating modeling

under the spiral has quite low flux density values. Therefore, the entire sample should be fitted in the gap in the middle (blank area in the middle of the spiral in the Fig. 7). As the result, the internal coil radius should be larger than 1 mm.

The third limitation increases the required current from 2 A to 7 A due to the small magnetic flux density values in the middle of the required area. For 7 A, the middle area magnetic flux value is 0.55 T, which is sufficient for the required task. The achieved geometry is given in Fig. 9.

2.5 Pulse length calculations

The following heating processes are modeled for the geometry that is shown in Fig. 9. The main idea of the calculation is to find the biggest pulse length that is still suitable for

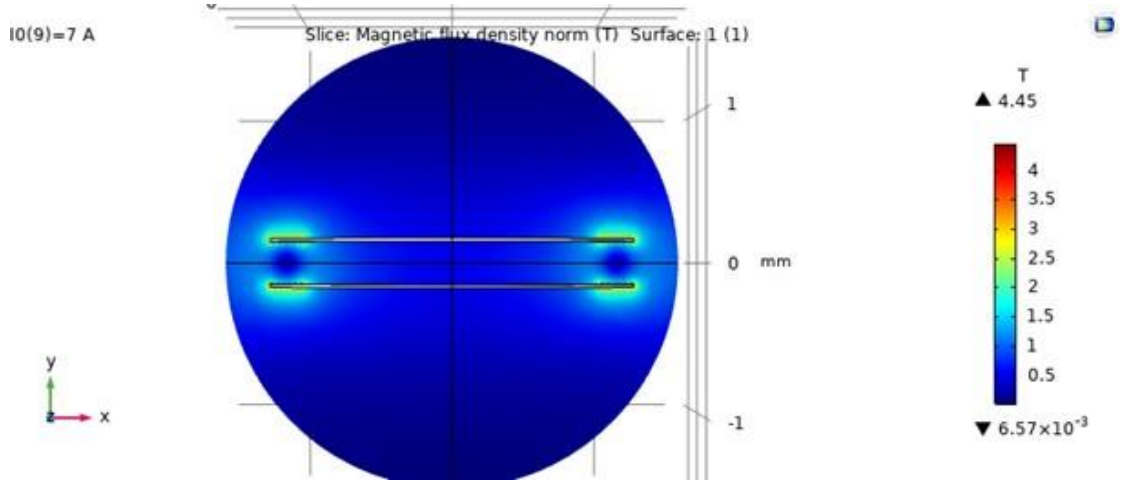

Figure 8. Model geometry and model results for required magnetic flux density value

the copper spiral. Fig. 10 presents the calculated temperature distribution of the coil and Table 2 shows the pulse lengths and corresponding coil temperatures.

Table 2. Spiral temperature for different pulse lengths.

Time t, ms	Temperature T, K	Temperature difference T, K
0.01	293.15	0.15
0.05	297	4
0.1	300	7
0.2	305	12
0.5	315	22
1	333	40

2.6 Conclusions

The coil geometry used in calculations is presented in Fig. 9. In this figure, current is equal to 7 A and pulse duration is 0.2 ms.

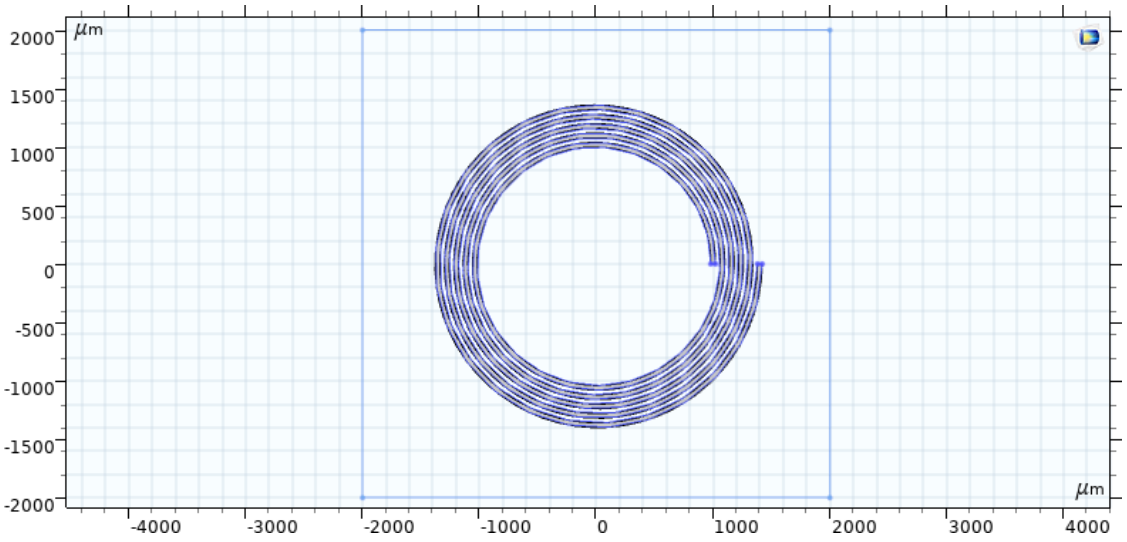

Figure 9. Calculated geometry

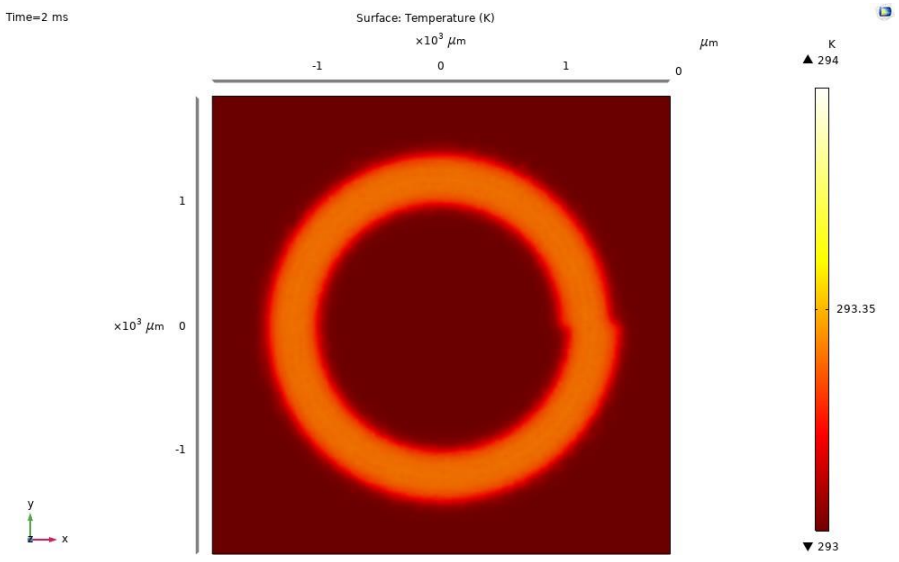

Figure 10. Modeling results for suitable a pulse length

3 Experimental part

3.1 Coil production

The model described in chapter 2 is verified with the following experiment. Copper coil is cut with a femtosecond pulsed laser micromachining system. The geometry of the coil is set via DXF format of image. This file format is a vector image format, and it allows to present the selected image in its initial dimensions without image quality loss. The geometry for the cutting process is slightly different than for modeling, mostly due to practical reasons relating to the laser machining. The first difference is the contact pads for the copper wire sattachment (Fig. 11). The second notable change in the coil geometry is change of the coil thickness. The coil in given geometry is 10 μm thicker than in the modeling and in the test sample.

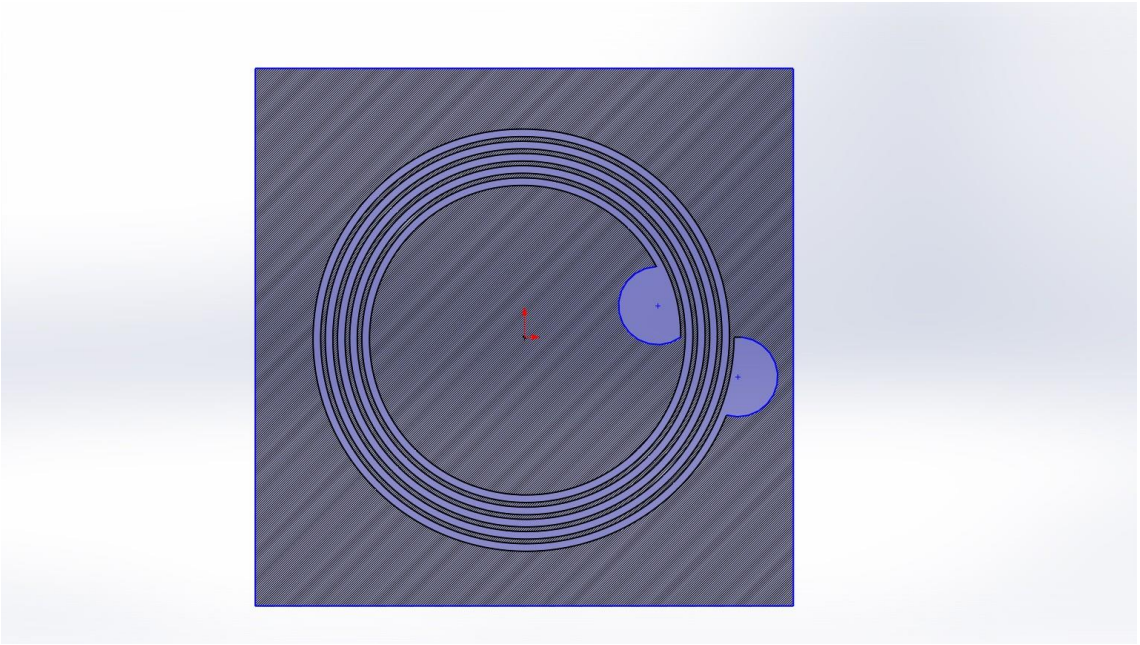

Figure 11. Geometry of the experimental copper coil

The cutting is performed using a femtosecond pulsed laser manufactured by Amplitude Laser with adjustable wavelength (1030 nm or 515 nm) and LS-Lab Access module [10]. The 515 nm ‘green’ wavelength was used due to its higher optical absorption to copper. The cutting process was first optimized by the laser operator. This was done to avoid process defects, such as melting on the edges or minor deformations.

Also, as it can be seen from Fig. 11, for the copper coil of 3 mm in width the manual coil detaching can damage the coil. Therefore, the coil geometry is reversed to what is expected to receive at the end of cutting. This geometry format is made to ablate the metal around the coil. For big enough coils (Fig. 12), cutting the edges is enough because it is easy to detach all extra copper manually. Also, extra thickness of the copper wires in the spiral is required due to the finite laser beam thickness. The laser beam evaporates all hatched parts of Fig. 11. As it can be seen from this figure, the laser beam is supposed to stop right before the copper spiral turn (there is no blank space between coil and the hatched area). As the result, laser beam may evaporate some coil parts on the "hatched area/coil" [11]. Current problem was solved by adding to the coil thickness 10 μm extra.Therefore, the manufactured coil has the same parameters: inner diameter is 2 mm, outerdiameter is 3.4 mm, copper coil thickness is 40 μm and gap between coil turns is 40 μm.

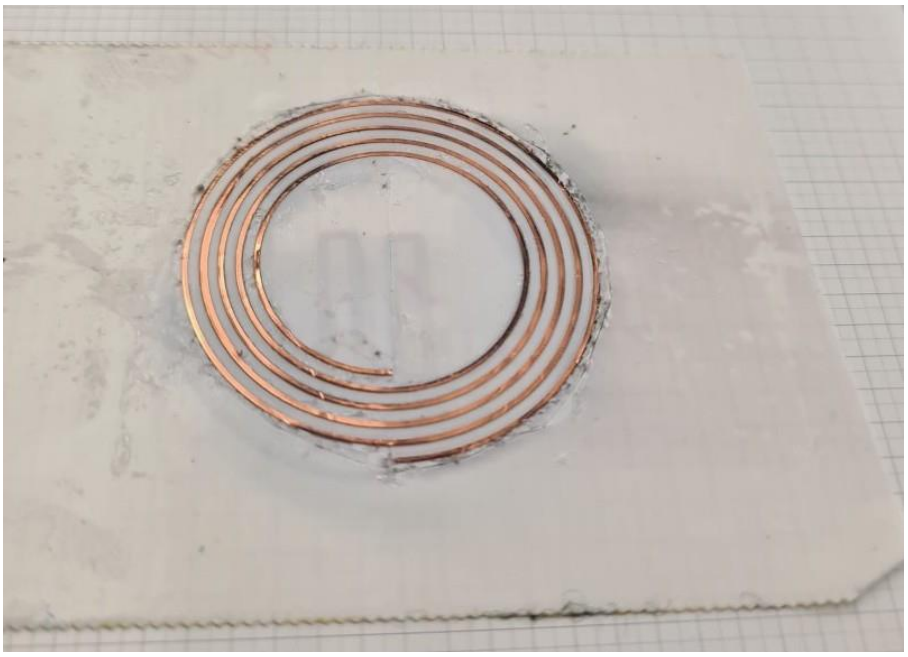

Figure 12. Experimental coil with outer diameter of 3.4 cm

The spiral was cut using femtosecond length pulses to enable cold ablation. The pulse length should be short enough to decrease the dissipating inside the copper material and it should be long enough to ablate the material directly without additional thermal effects to the processed material. The copper coil cutting result is presented in Fig. 13. According to the coil parameters measurements, the coil geometry is the same as it is shown in chapter 2 (except for pads for soldering, Fig. 11). Therefore, this sample can be used to verify calculations accuracy.

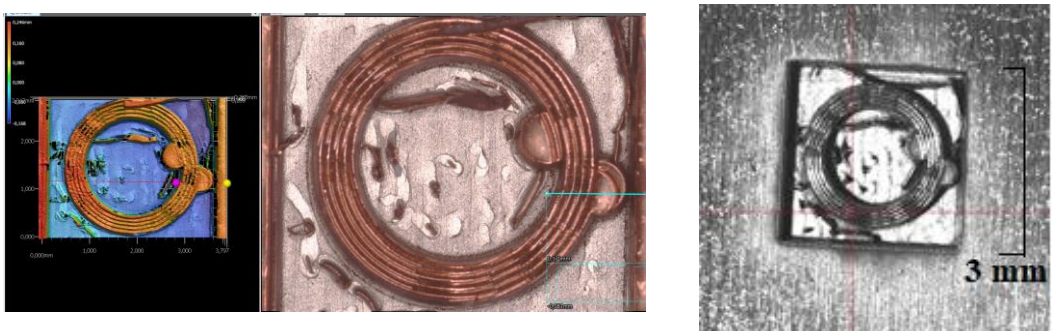

Figure 13. Microscopic images of the laser cut copper spiral

The next step is to control the coil quality and dimensional accuracy and to prepare the samples for the measurements of coil parameters. It is also good to have more than one sample for the testing for the case if the first sample were damaged. The first preparation step is to provide proper mechanical support to reduce coil damage. The second step is to attach the connection wires for this spiral which may be quite tricky because of the small coil size.

In chapter 2, geometry was calculated mostly for the photolithography manufacturing method (which is more precise but also more expensive). This method allows to obtain a multi-layer system for the designed geometry. As the result, soldering pads can be transferred to the different layer for the better contact and soldering convenience. However, for the current production type the geometry is too small. Quite close position of the coil turns causes spiral to collapse as soon as the mechanical pressure is applied. This problem and the problems that occur due to the limited accuracy of the laser manufacturing process are the main reasons to scale up the system until it is large enough for soldering the coil manually. The system is scaled up gradually. The entire geometry is enlarged by 2 mm up to 6 mm for copper coil outer diameter. During this procedure, all parameters are increased accordingly. In this system coil width, coil gap and both inner and outer diameters enlarge by the same value and their proportions are the same as they were calculated in chapter 2. According to the method described above, the minimal copper coil outer diameter is 5.6 mm. The final geometry to be cut is presented in Fig. 14. This figure has an additional circle in the middle to simplify the soldering process. The circle is turned away from the sample surface and the wires are soldered to these turned parts.

The inner diameter in this geometry is equal to 4 mm, the copper width of one turn is

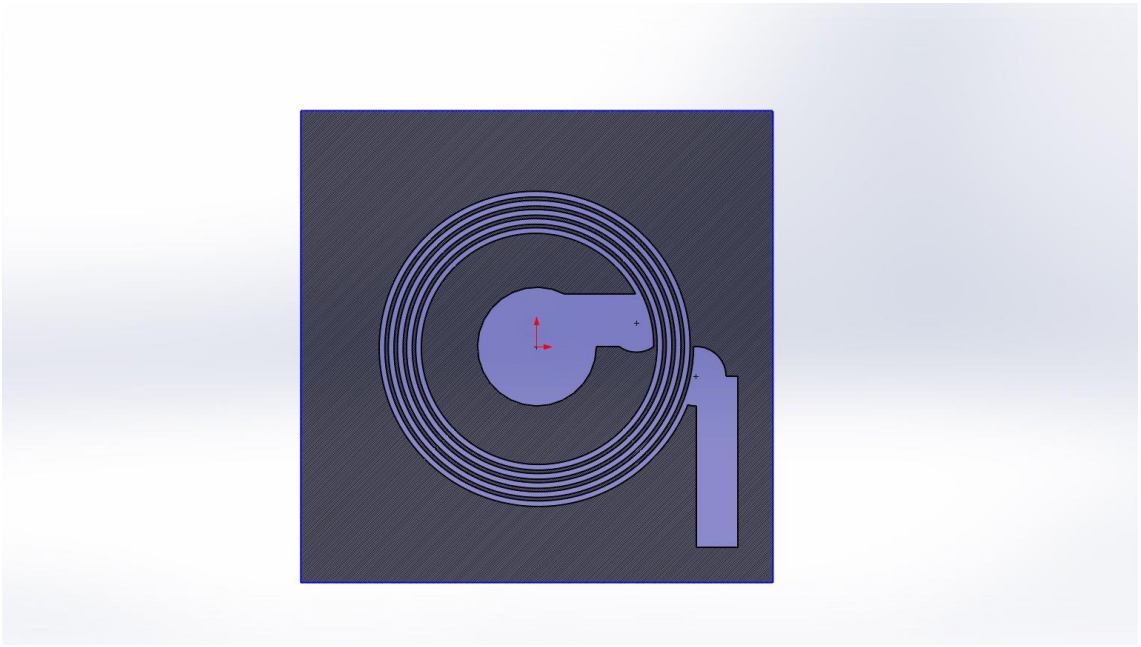

Figure 14. Geometry for experimental coil with outer diameter 5.6 mm

80 μm and the distance between spiral turns is also 80 μm. According to the experimental results, this is the smallest gap between coil turns that the used laser system can provide. The difference in quality between the copper coils can be seen in Fig. 15 and Fig. 16.

As it can be seen in Fig. 15, the image of the larger copper coil has significantly less defects. There are no cuts on the surface or uncut parts unlike the copper coil with the smallerouter diameter. For the experiment, four copper coils were prepared (Fig. 17).

Another difference to the smaller geometry is cutting on a different substrate. The old substrate used the adhesive tape to attach the copper foil to the substrate. The larger copper coil geometry was cut on the glass substrate and was glued without the sticky tape (Fig. 16).

To compare the experimental model, it is required to recalculate the expected flux density and the coil heating for the produced coil geometry. Using the same model, it was shown that it is required to apply 20 A to get the same flux density (0.63 T). At 7 A, the current geometry creates 0.31 T. This value is too small for the purposes mentioned above. Therefore, it was necessary to increase the current from 7 A to 17 A, because it is the smallest current value that is required to get the magnetic flux density higher than 0.5T (Fig. 18).

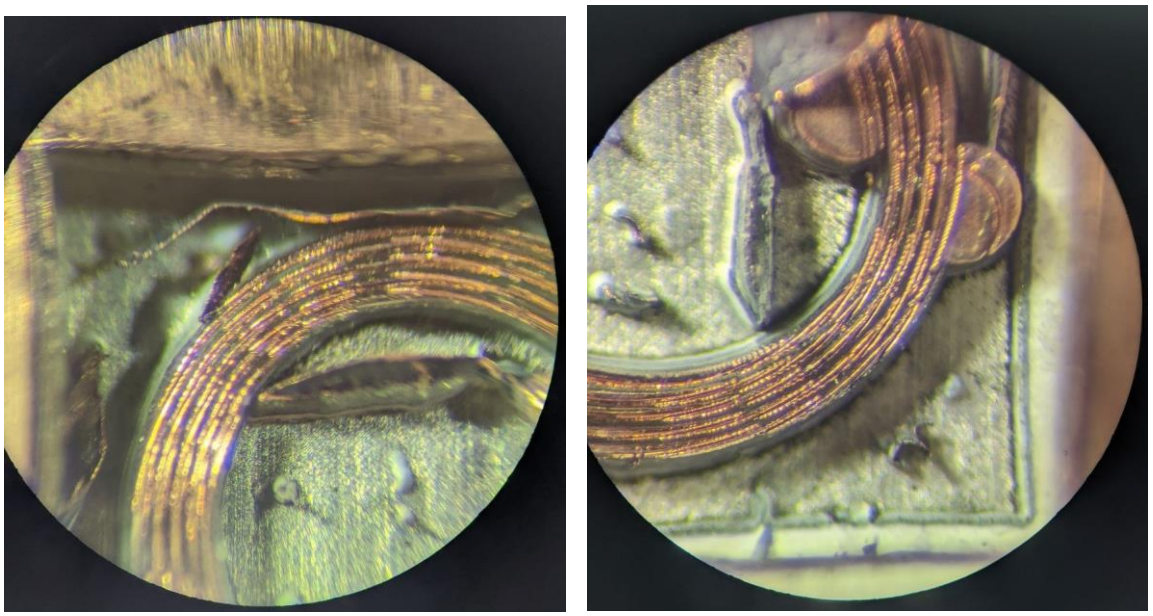

Figure 15. Cutting results for the copper coil with the outer diameter of 2.8 mm. (a) Microscope image of the first test coil; (b) Microscopic image of the second test coil.

The changes discussed above require the pulse length recalculation. For these purposes, the second calculation model was used. The higher the current is, the smaller duration of the pulse and more time for cooling of copper is required. As the result, minimal duration of the pulse frequency is 0.1 ms (Table 3). This value is small enough to avoid strong heating of the coil and to enable high operation frequencies. The results of the heating of the copper coil are presented in Fig. 19.

Table 3. Coil temperature for different pulse lengths for 17 A.

Time t, ms	Temperature T, K	Temperature difference T, K
0	293.15	0
0.1	297	3.85
0.2	298	4.85
0.3	301	7.85
0.4	303	9.85
0.5	305	11.85
0.1	305	11.85
1	314	20.85
1.5	323	29.85
2	331	37.85

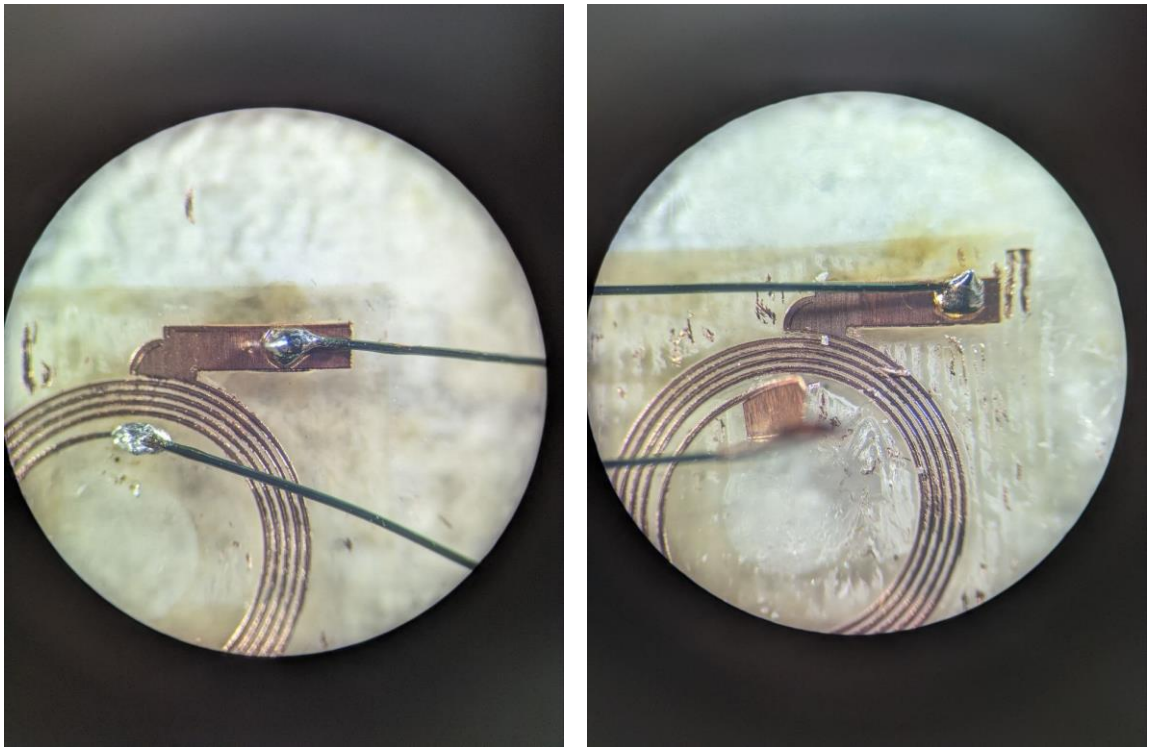

Figure 16. Cutting results for the copper coil with outer diameter of 5.6 mm. (a) Microscopic image of the first test coil; (b) Microscopic image of the second test coil.

3.2 Coil parameters measurement

The main purpose for fabricating the coils is to verify the model. Therefore, it is required to measure the magnetic field strength or magnetic flux density. Also, it is useful to see if the coil can be used for this pulse duration. Hence, it is necessary to measure how high temperature the given pulse duration raises. Also, it is worth measuring how coil heating affects the magnetic field and what time it takes to cool the coil down. The first part of the measurements is the induced magnetic field measurements. For these purposes, Hall detector (figure 3.5) was used. All further measurements were conducted only for one coil, as the Hall sensor is too big to fit in the gap 0.3 mm between two copper coils, as it was shown in chapter 2. The detector is supposed to be placed in the empty area inside of the coil.

The experiment has some differences from the modeled geometry. The first and the most important difference is the substrate. While modeling is performed in the air, the experimental sample is attached to the glass substrate via glue substance. The substrate affects the temperature dissipation and may affect the maximum pulse duration.

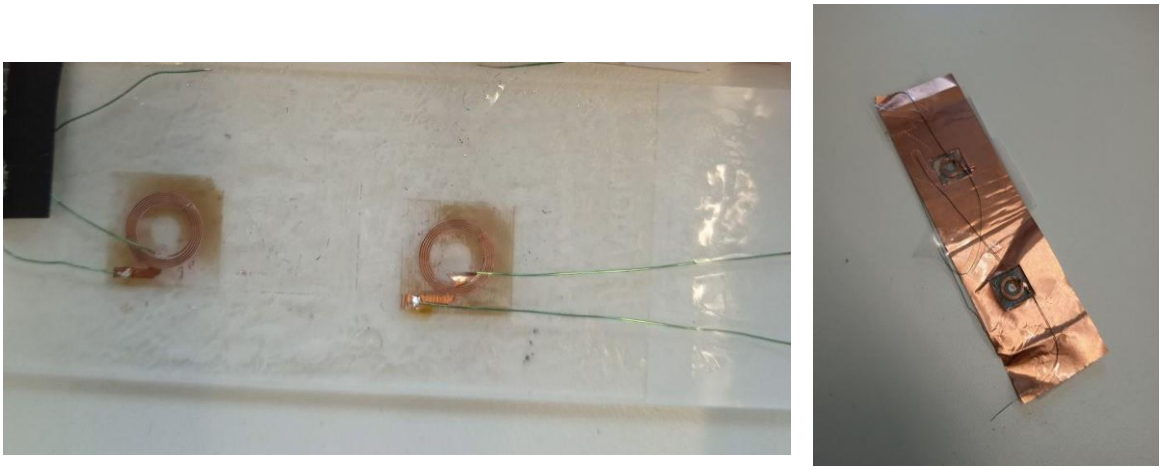

Figure 17. Copper coils used in experiments . (a) Mmicroscopice image of the coil with an outer diameter

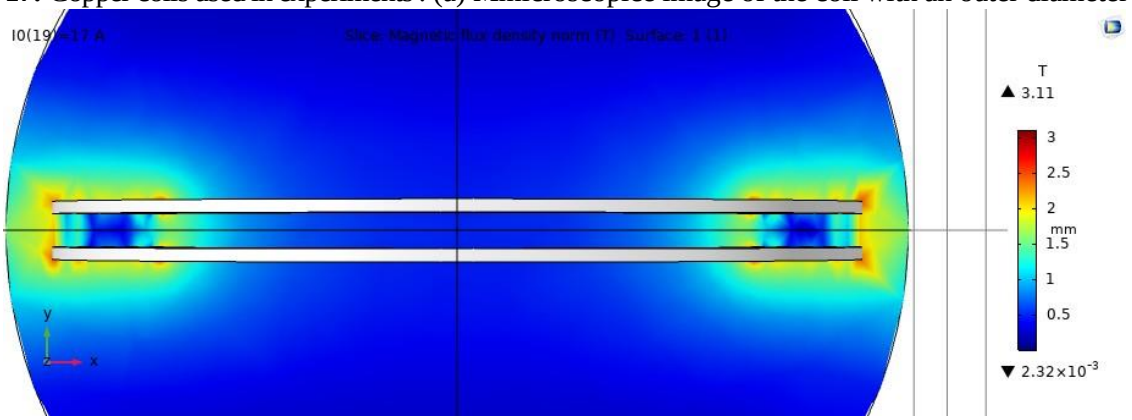

5.6mm (samples 3 and 4), Microscopic (image of the coil with an outer diameter 5.6mm (samples 1 and 2)**Figure 18.** Calculated results of the magnetic flux density for the copper coil with an outer diameter of 5.6 mm.

Moreover, too large current pulse can cause the electrical breakdown. In this case, the current does not follow the copper coil geometry but conducts the current via the substrate. In this case, the magnetic field is not created at all.

Another quite large possible impact on the experimental results is the change of the geometry due to the soldering process. The different (usually higher) resistance may cause additional heating in the contact places (soldering pads). The wires were additionally fixed near the coils by epoxy resin before the measurements were performed. The coils are numbered as shown in Fig. 20. The short (100 microseconds long) pulse was conducted through the copper coil.

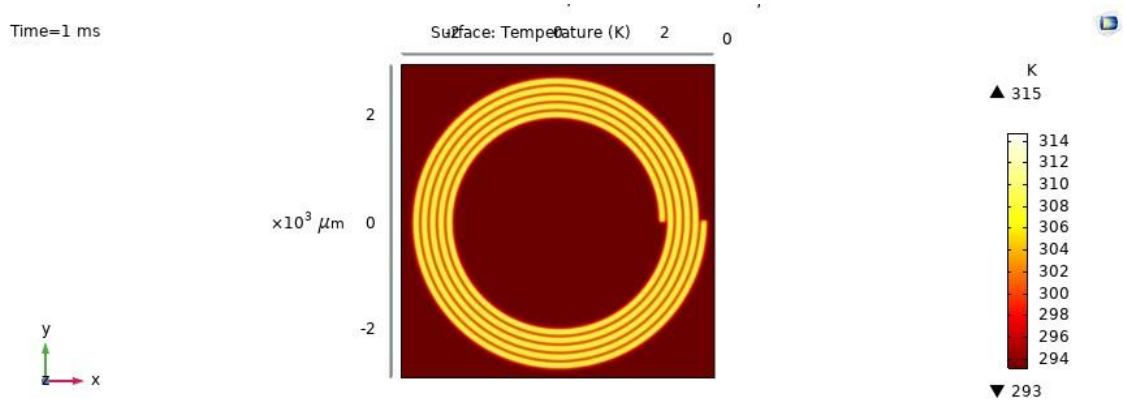

Figure 19. Calculated heating of the copper coil with an outer diameter of 5.6 mm

The current appliedwas approximately 6 A. For these conditions volt-ampere characteristics were obtained. After the recalculation, these results were used for electrical resistance from current and electrical resistance from the time dependencies building (Fig. 22 and Fig.23). Some coil imperfections appeared to lead to the magnification of the coil as shown in Fig. 21.

Additionally, all the measured coils have different resistances. For showing the effect, all the graphs are plotted at the same Figure 20. The results of the measured characteristics are presented at the next section.

3.3 Results discussion

Following figures present the dependency of the resistance on time, where the first moment of the pulse corresponds to the start of the current application. This section containsthree graphs with volt-ampere characteristics, resistance from the current characteristics and the time dependency resistance.

Fig. 22 shows measured resistance from temperature dependency. As it can be seen from the figure, the dependency is highly nonlinear. This non-linearity is explained by change of the current inside the coil. The main idea of this graph is to show when the coil is heated most. The higher resistance value corresponds to higher heating. As the result, the highest heating is at the rising and falling parts of the signal. Therefore, the shape of the input signal also significantly affects both coil heating and the produced magnetic flux density.

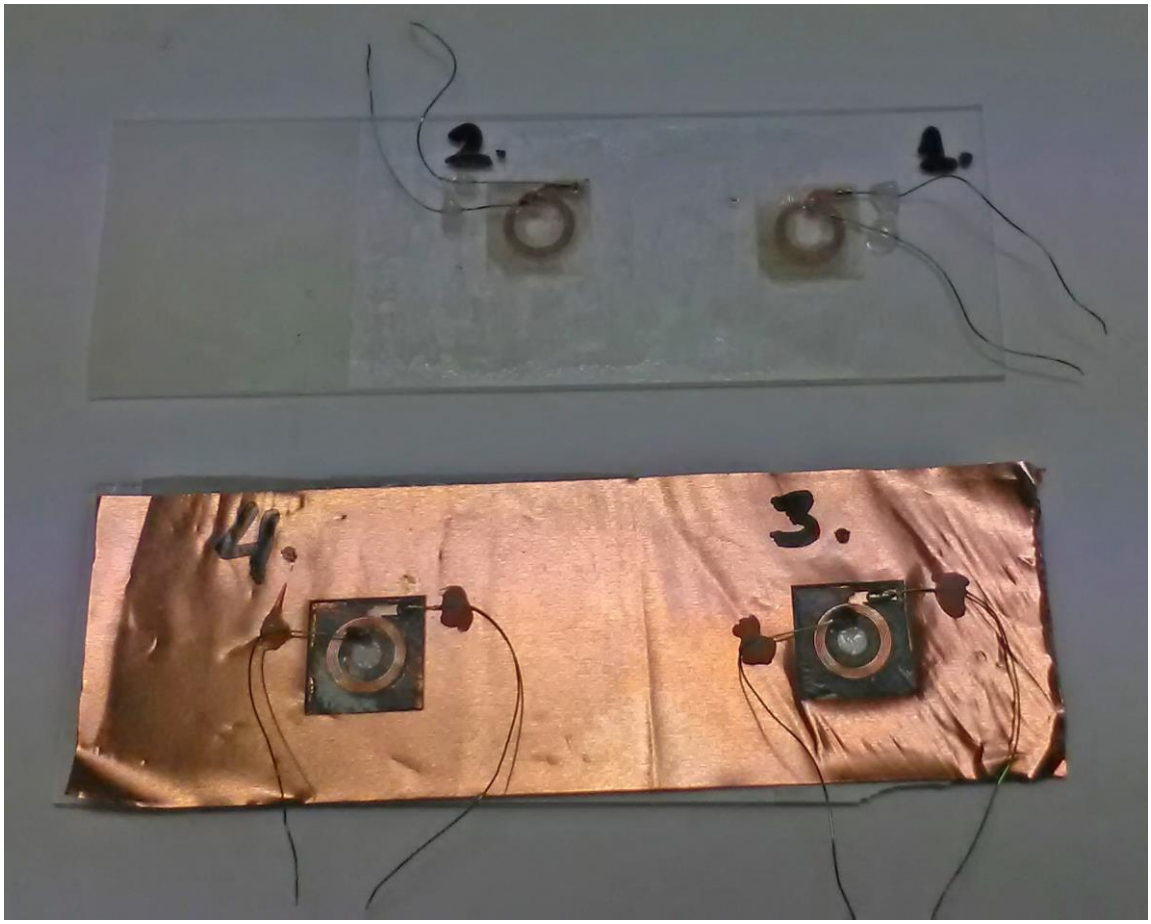

Figure 20. Preparations for coil parameter measurements

Figure 23 shows the resistance experimentally obtained from the current dependency. This dependency is non-linear. The graph helps to visualize the experimental resistance obtained from current dependency. Also, this graph supports the statements that were made for Fig. 23. The studied graph shows the dependency of heating on the current in the calculated system.

The next experimental graph is the Volt-Ampere graph (Fig. 24). As it can be seen from the graph, all the studied copper coils have different resistance, eventhough all four test subjects have the same geometry. The main reason is the difference of metal that was used for soldering. This difference may influence heating properties of the coil. The main way to decrease this discrepancy is to change the way of coil production. The suggested new design supposes the specialized pads for soldering, which are taken away from the working area.

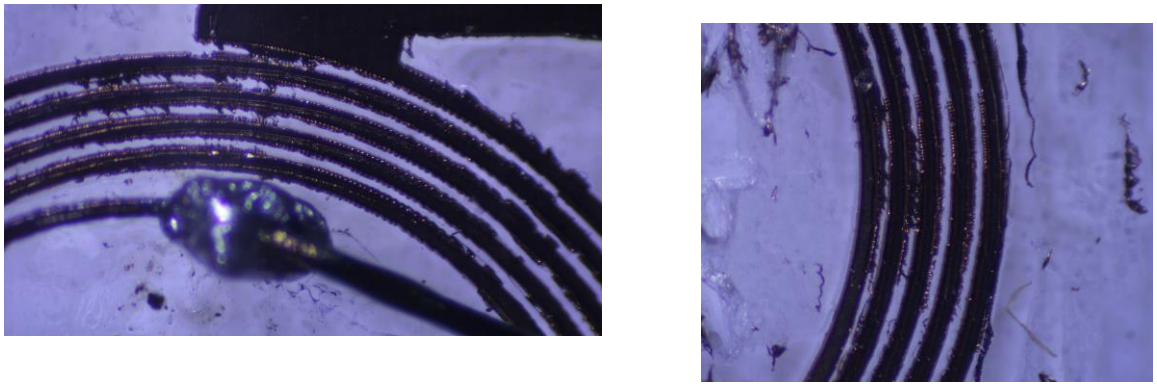

(a) (b)

Figure 21. Coil state after measurements

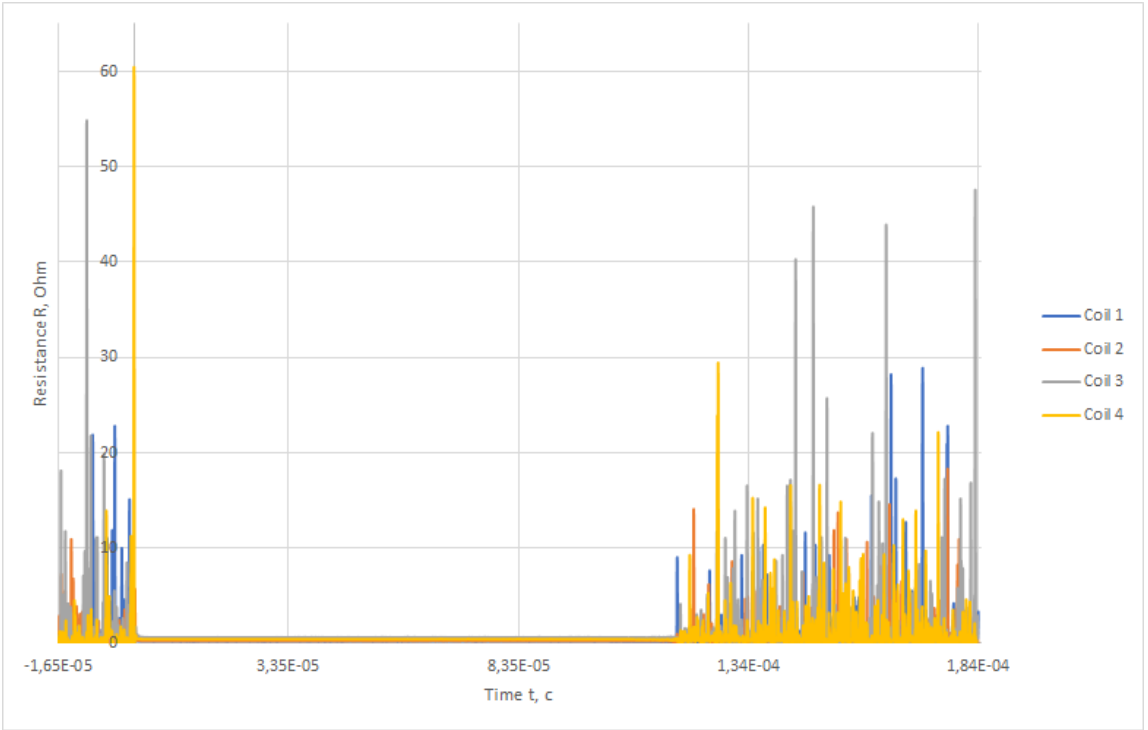

Figure 22. Resistance from time dependency for test coils

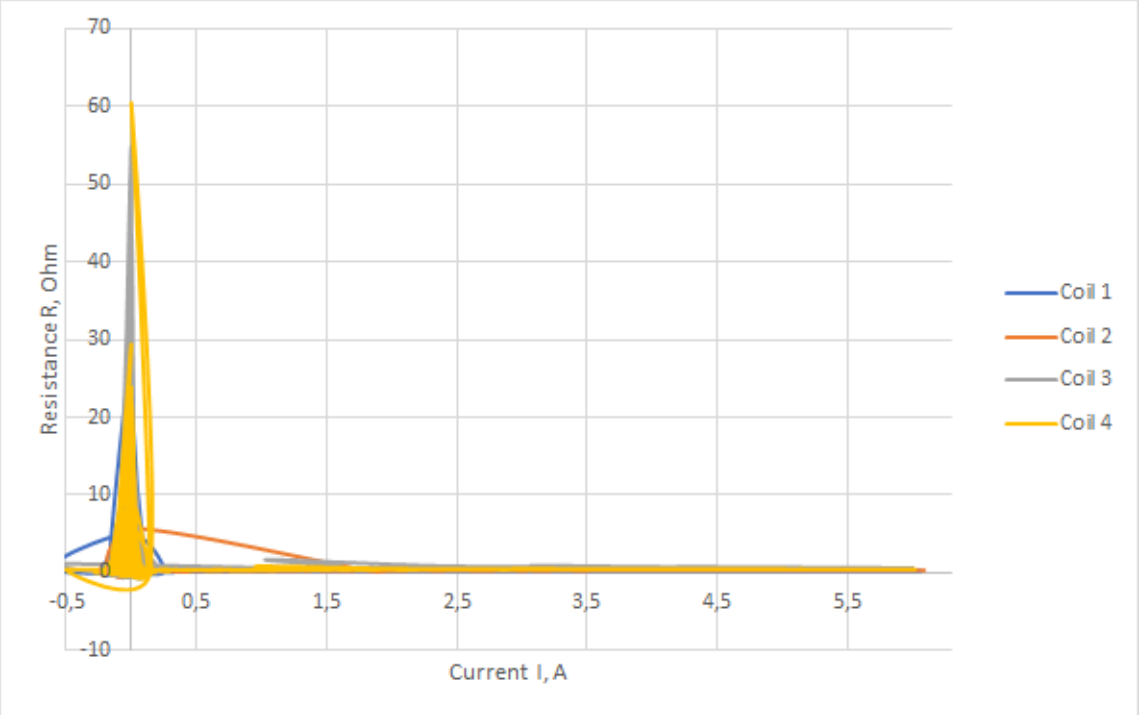

Figure 23. Resistance from current dependency for test coils

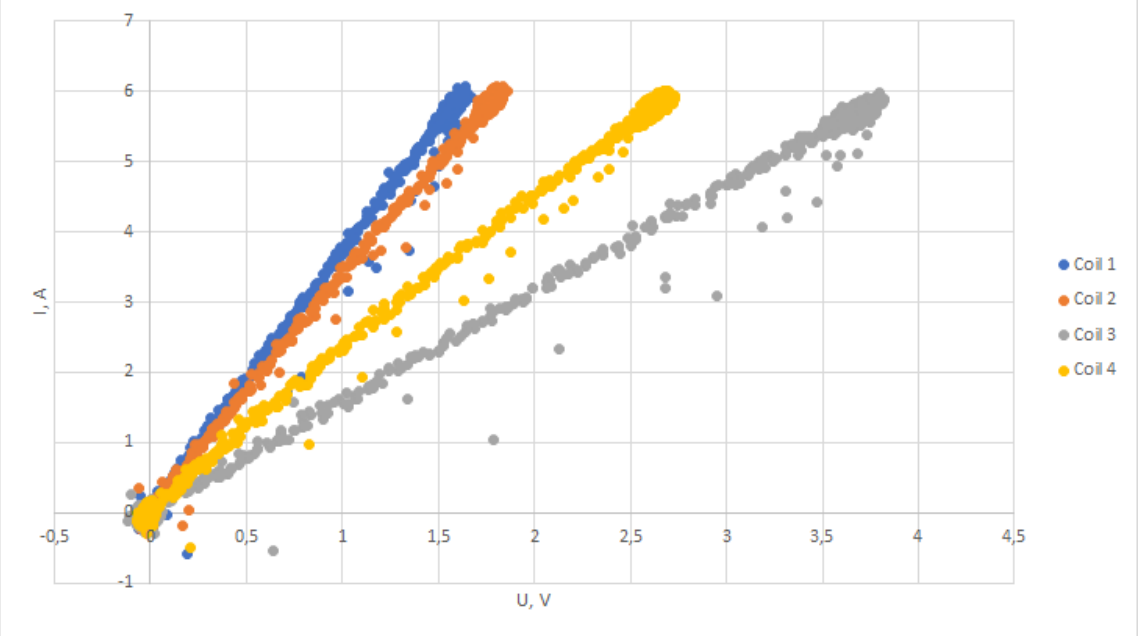

Figure 24. Volt-Ampere dependency for the test coils

4 Theoretical calculations

4.1 Study of the effect of the main geometry parameters on the magneticflux density

The designed geometry is based on the Archimedes' spiral geometry. This is a geometrical curve, which has even distance between the turns. This curve has several parameters that describe the geometry characteristics. There are five main parameters. The first one is the inner diameter. This parameter defines how big the working area is. The second parameter is the outer diameter. This parameter defines how big the coil is. The third parameter is the number of turns. The fourth parameter is the width of the copper coil turn. The fifth parameter defines how small is the distance between copper coil turns.

Another important parameter that is not connected to the surface geometry is the copper coil thickness. It is required to study all the mentioned above parameters to be able to forecast the geometry change. However, study of the outer diameter of the coil is less informative than the study of the gap between the curves on the created magnetic flux density, because the outer diameter growth also causes growth of the other studied parameters. All the following studies are based on the same models that were described in chapter 2. The studies are performed for the inner diameter of 2 mm, for the copper coil turn thickness of 40 um, and the distance between turns of 40 μm. It is also assumed that there are turns for 2 coils that are placed at a distance of 0.3 mm from each other. All the calculations are performed for current of 7 A.

The first studied parameter is the inner diameter. The graph presented in Fig. 25 shows the dependency of the magnetic flux density on the inner diameter of the coil in the middle of the working area of the coil. Inner diameter is changed from 40 μm to 1.5 mm. As it can be seen in Fig. 25, the larger inner diameter is, the smaller magnetic flux density is. This effect is explained by the extensive decay of the magnetic field strength with the increase of the distance from the wire. Therefore, it is required to decrease the working area to the smallest possible value to increase the system efficiency. Quite similar situation is also for the dependency of magnetic flux density on the gap between the coil turns (Fig. 26). Nevertheless, the effect from magnetic flux density decay with the gap between the coils increase is smaller than the effect that is caused by inner radius growth. This effect is explained by the fact that the closest coil remains at the same distance. Therefore, the most of the magnetic flux density that is created by the closest turn remains unchanged.

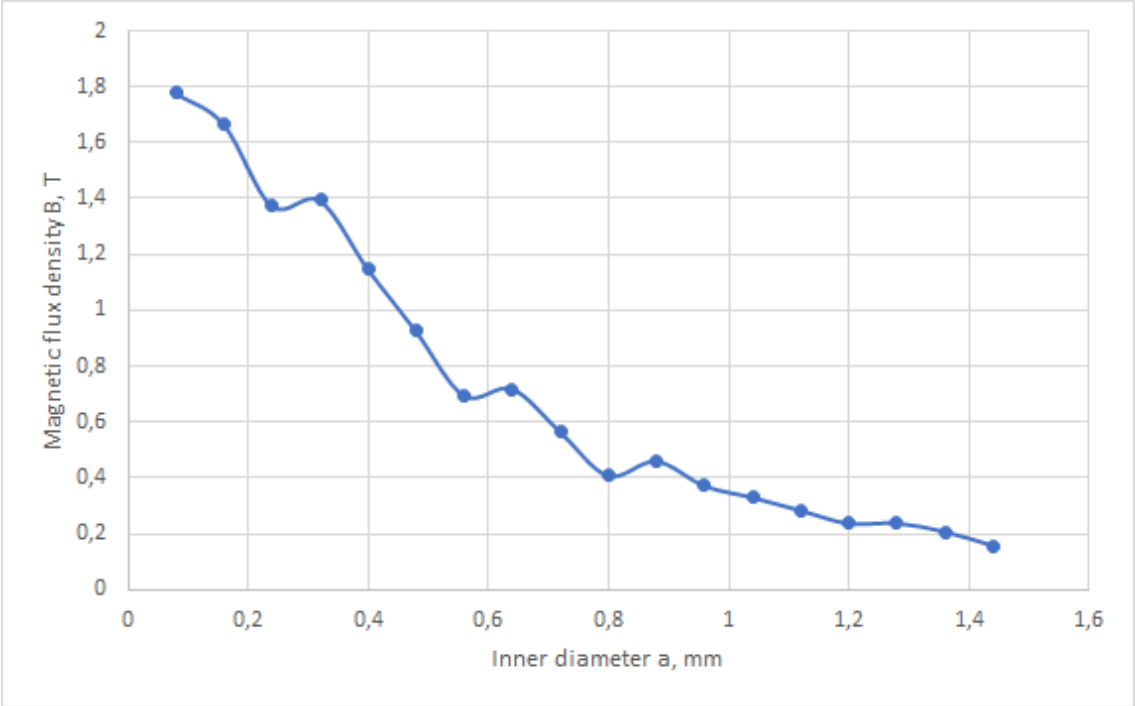

Figure 25. Dependency of the magnetic flux density on the inner diameter of the coil.

The next studied parameter is the copper coil thickness. Fig. 27 presents the modeling data for the copper spiral with 5 turns, where the only changing parameter is the thickness of the turns of the coils. As the result, the further copper coil turns appear to be further from each other than they used to be for the thinner copper coil turns. As it was shown in Fig. 26, such a shift may cause the additional decay that has nothing to do with an actual magnetic flux density decrease. To separate these two studied parameters, it is required to study the same dependency for only one (the closest one) copper coil turn. This type of dependency is not affected by the distance between the coil turns and, hence, is more precise. The results are presented in Fig. 28.

The same type of dependency is achieved with increasing the copper coil thickness, as the main parameter here is the area of the conducting part which affects the current density.

As it can be seen from Fig. 28, the magnetic flux density at first decreases. The copper coil magnetic flux density decay is explained mostly by the decrease of the current density inside the coil, as the current remains unchanged while the conducting surface is increased.

The next studied parameter is the number of turns. Fig. 29 presents the dependency the magnetic flux density on the number of turns. As it can be seen from this figure, the magnetic field strength has nonlinear dependency on the number of coils. The

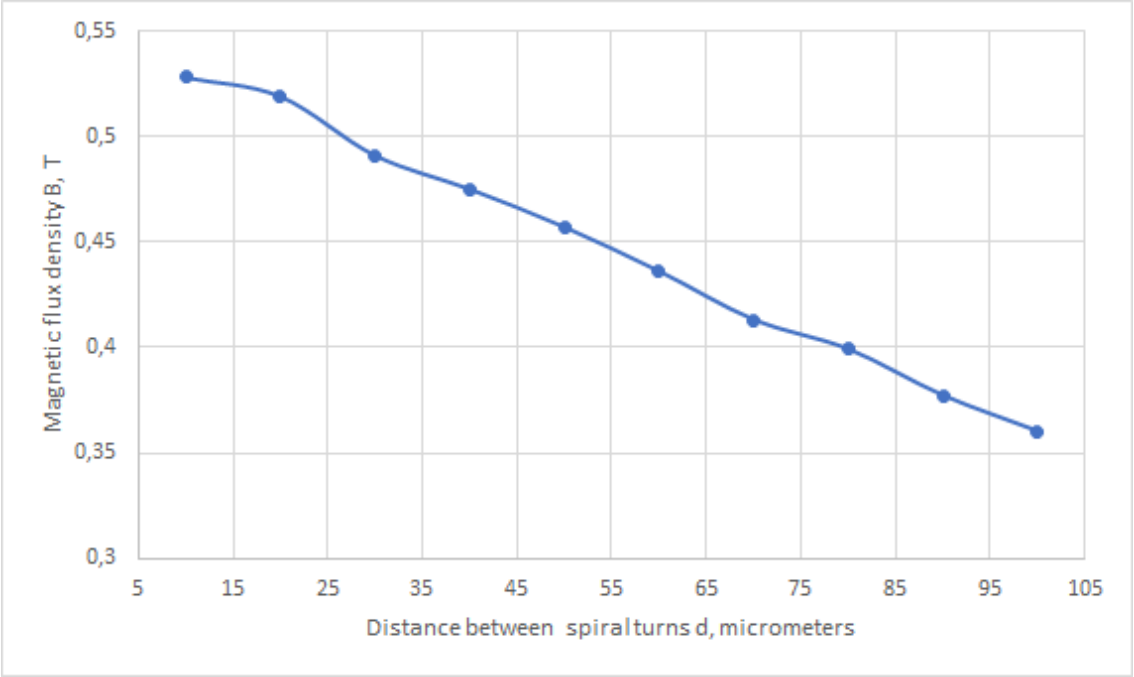

Figure 26. Dependency of the magnetic flux density on the gap between the turns of the

Dependency behaves like $y = a*x^{0.5} + c$ function, where a and c are constant real numbers. This dependency shows that it is impossible to reach the required flux density by adding turns to the coil. The most effective number of the turns for the coil can be found in Fig. 30. The most optimal number of turns is equal to 5. The flux density growth (9 percent) is too lowto compensate the additional technological difficulties that are connected to the increase of the number of turns.

As the result, the most effective coil that creates the required flux density is the composed of 5 or 6 thin turns. The distance between these turns is supposed to be minimal.

The second step in the study of the input parameters is to find how their (input parameters) change affects the system heating. For these purposes, the second model presented in chapter 2 was used. The initial parameters that are not varied during the study are the same as for the first model: inner diameter of 2 mm, outer diameter of 2.8 mm, 5 turns of coil, both the thickness of the coil turn and the gap between the turns are equal to 40 μm. The system is studied for the current of 7 A and the duration of 5 ms.

The first studied parameter is the inner diameter. The discussed dependency is built for the working spaces from 80 μm up to 1440 μm. Corresponding temperature dependency is presented in Fig. 31.

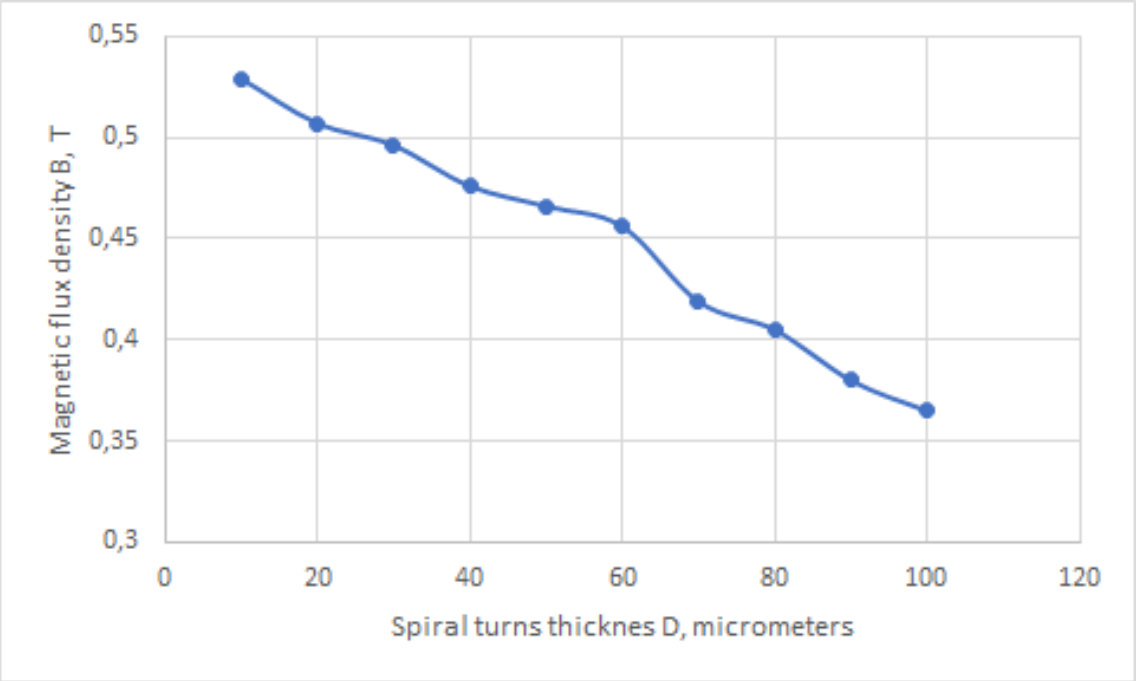

Figure 27. Magnetic flux density vs. thickness of the turns of the coil.

As it can be seen from the graph, temperature has highly nonlinear dependency on the inner diameter. This type of dependency is explained by the nonlinear dependency between the coil size (its length) and the increase of the inner diameter. This non-linearity and the temperature increase itself can be approximated by the black line in Fig. 31. As it can be seen in Fig. 31, the increase of the inner diameter has a noticeable impact on the copper coil heating. A 5 millisecond pulse heats 2.4 K more the spirals with a larger radius than the ones with the smaller one.

The second observed parameter is the dependency of the copper coil heating on the distance between the coils. This parameter is varied from 10 to 80 μm with steps of 10 μm. The studied dependency is presented in Fig. 32. As it can be seen from the figure, at first the temperature decreases to the minimum value of 365 K during a 5 millisecond pulse. Then the coil heating increases for the same pulse duration. This minimum can be explained by two mechanisms that are affecting the temperature increase.The left side of the graph goes down due to the decrease of the influence from the neighboring coil turns on each other heating. For these coil geometries, the closer copper turns are, the more they are heated from each other. However, as coils go further from each other, the coil length grows accordingly. At the coil gap of 140 μm, the influence from the growth of the coil length becomes higher than the effect from the decrease of the heat from the neighboring coil turns. As the result, further gap between the coils increases its heating.

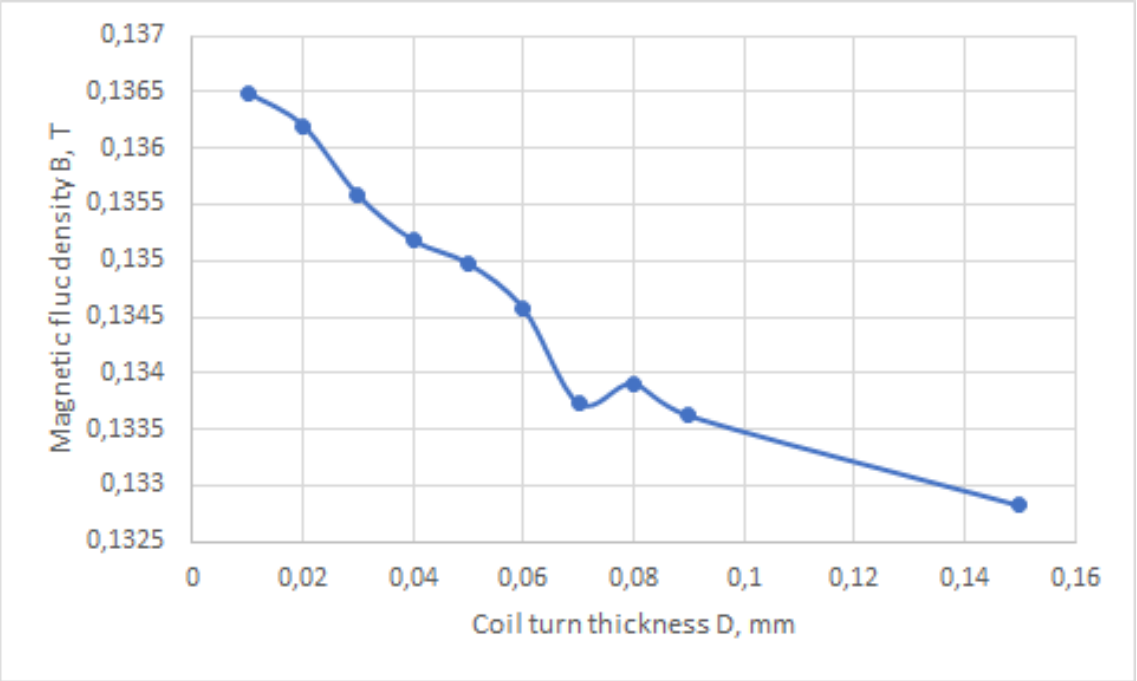

Figure 28. Magnetic flux density from copper coil thickness dependency for 1 turn spiral

The next studied parameter is copper coil width. This parameter was varied from 10 to 80 μm. Modeling results are presented in Fig. 33. As it can be seen from the graph, the wider turn of the copper coil heats less than a thin turn. This effect is the consequence of the same process that can be seen in Fig. 27. Decrease of the current density leads to less amount energy spent on heating. However, it is worth considering that temperature decreases with the increase of the width of the turns highly nonlinearly for 5 millisecond pulses. Therefore, it is highly inefficient to increase this parameter. It is sufficient to increase the turn width up to 30 μm.

The next studied parameter is the number of turns. Number of turns in this study is varied from one to 6 turns. The results of modeling are described in the Fig. 34. As it can be seen from the graph, increase of the turns of the coil increases the coil heating. The studied dependency is highly nonlinear. From Fig. 34 it is obvious that there is no point to decrease the number of the turns to decrease the heating process.

However, it is worth considering specific geometry type with only one copper coil. This type of geometry is easier for production and the system can be scaled down to the much lower dimensions. The proposed geometry will be modeled in this chapter in paragraph 4.4.

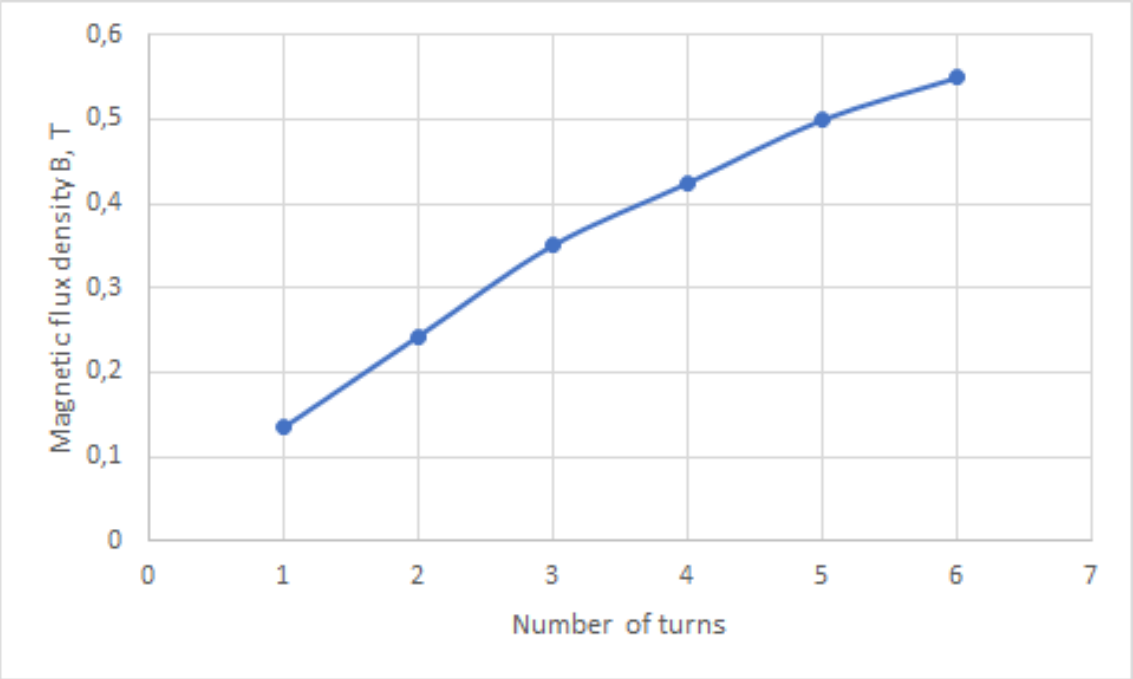

Figure 29. Magnetic flux density from number of turns dependency

As the result, the main limiting factor for system scalability is the MSM sample size. This value affects the inner diameter. It is also required to scale down the width of the turn of the coil and to set the gap between the coil turns to the value where the magnetic flux density and the system heating are brought to the optimal ratio.

4.2 Theoretical calculations for system scalability

It is required to determine the system scalability. Therefore, this part of study is devoted to the determination of the smallest possible coil size that could be obtained. This calculation model is based on the model from chapter 2. This geometry is not supposed to contain any Ni-Mn-Ga sample with a specific size. Therefore, the calculation system model is modified as it is shown in Fig. 35 and Fig. 36.

Main numeric parameters of the coil size are limited by the coil production process. The most precise method of the coil production is photolithography. This type of lithography is limited to the 100 nm [12]. This value is the smallest length that is possible to obtain precisely. Etching processes in photolithography demands that minimum distance should be increased at least 2 times. Therefore, the minimum copper width is supposed to be 0.2 μm at least. It is also important to remember about the copper spiral endurance. According

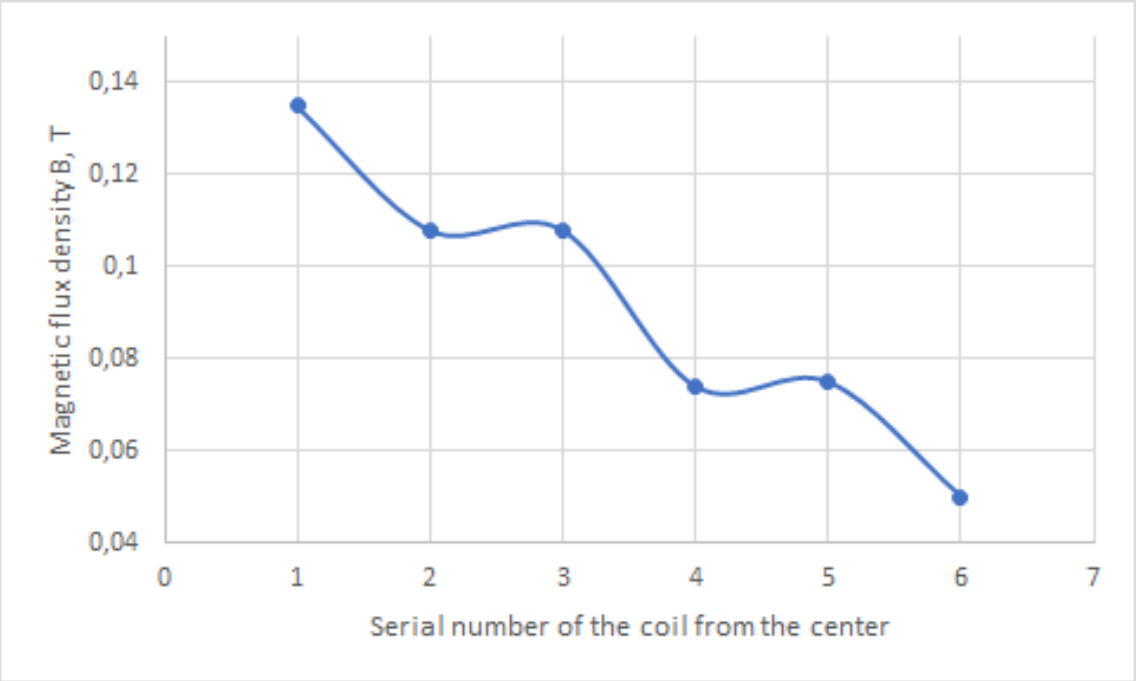

Figure 30. Magnetic flux density for each coil turn

to the parametric sweep for the spiral geometry (Table 4) minimum current value is equal to 0.5 A. Following Tab. 4 presents the comparison of the received dependency from current table with the coils from chapter 2. The only difference with the performed earlier calculations is that the distance between the two coils is equal to 15 μm instead of 150 μm that was used earlier. All the numbers are presented in Table 4.

Table 4. Dependency of magnetic flux density B on current.

Magnetic flux density (new) B, T	Magnetic flux density (old) B, T	Current I, A
1.04	0.041	0.5
1.45	0.058	0.7
2.09	0.084	1
4.14	0.168	2
6.2	0.253	3
8.28	0.335	4
10.44	0.421	5
12.53	0.502	6
14.498	0.59	7

Following graph (Fig. 37) shows that smaller values of the current are enough to create large enough flux density value B. This effect is explained by the heavy dependence of the

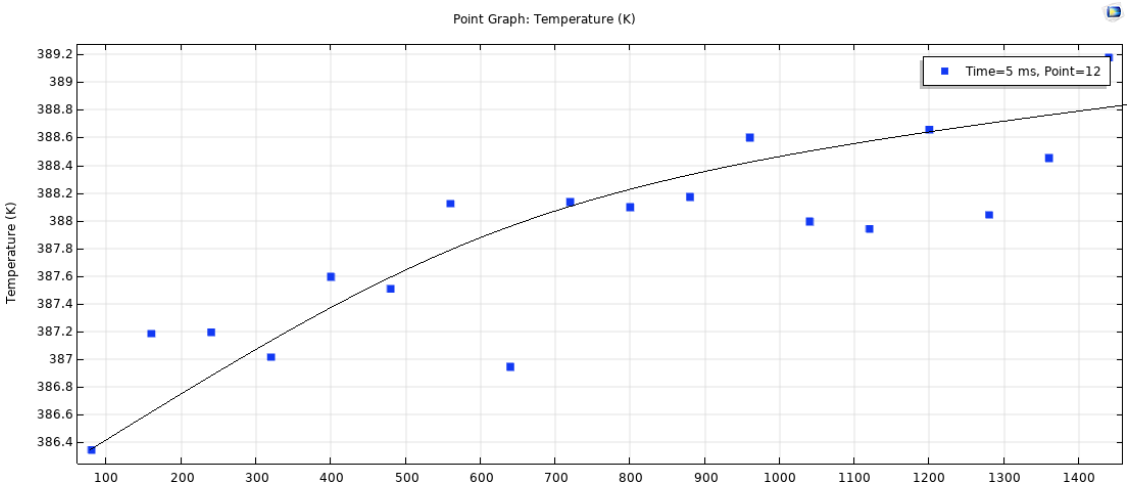

Figure 31. Coil heating vs. the inner diameter of the coil (in μm).

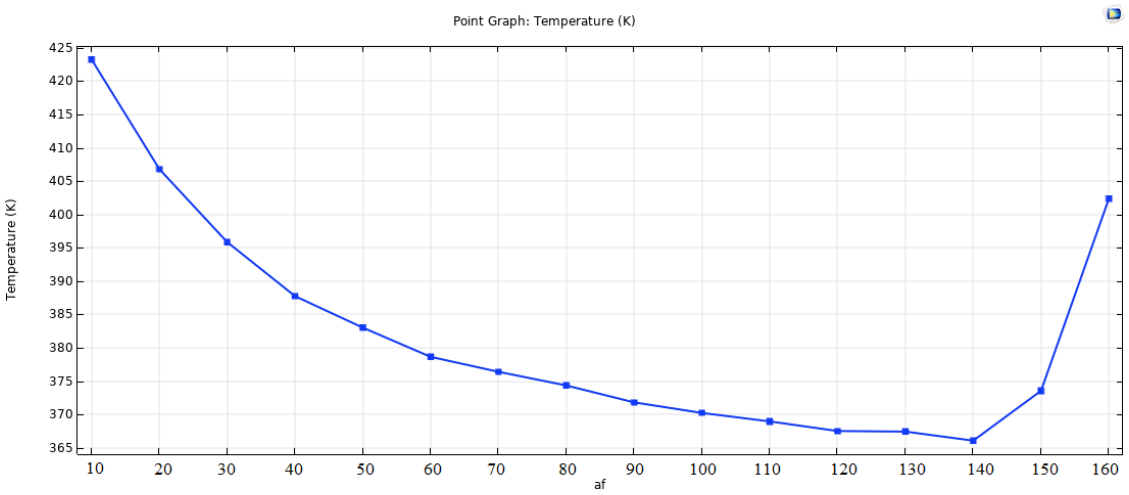

Figure 32. Coil heating as a function of the gap between the turns (in μm)

magnetic field discrepancy on distance from the current source. Therefore, the greater distance from the copper coil requires more current to create required B value.

The copper endurance is mostly defined by copper heat conductivity. This parameter is calculated mostly in the second model (Fig. 38). This model is described in chapter 2.

Following table contains temperature dependency for the copper spiral of a given geometry model and for the current of 0.5 A. This current value is large enough to create the required magnetic flux density.

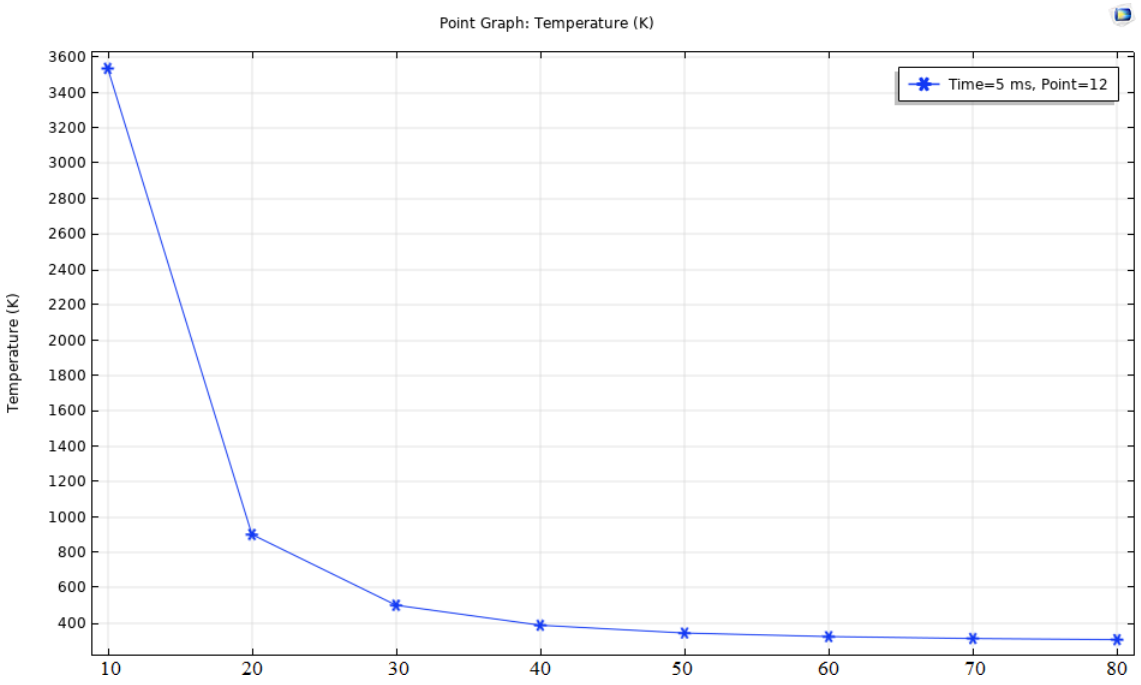

Figure 33. Coil heating vs. the width of the turn (in μm).

Table 5. Spiral temperature for different pulse lengths.

Time t, ms	Temperature T, K	Temperature difference T, K
0.01	293.15	0.15
0.05	294	1
0.1	294.4	1.4
0.2	295	2
0.5	296	3
1	296.5	3.5

4.3 Model calculation for different coil geometries

All the previous coil geometries assume that the Ni-Mn-Ga sample has comparatively similar dimensions. Therefore, it is required to calculate the magnetic field distribution for systems, where coil length is larger than coil width. For these purposes model with a geometry shown in Fig. 39 was created. The modeling results are presented in Fig. 40 and listed in Table 4. All of the numbers are taken from the middle of the area between two coils. As it can be seen from Table 4, oval-shaped spiral is more effective for long and thin samples of Ni-Mn-Ga. This geometry allows to use smaller values of the current.

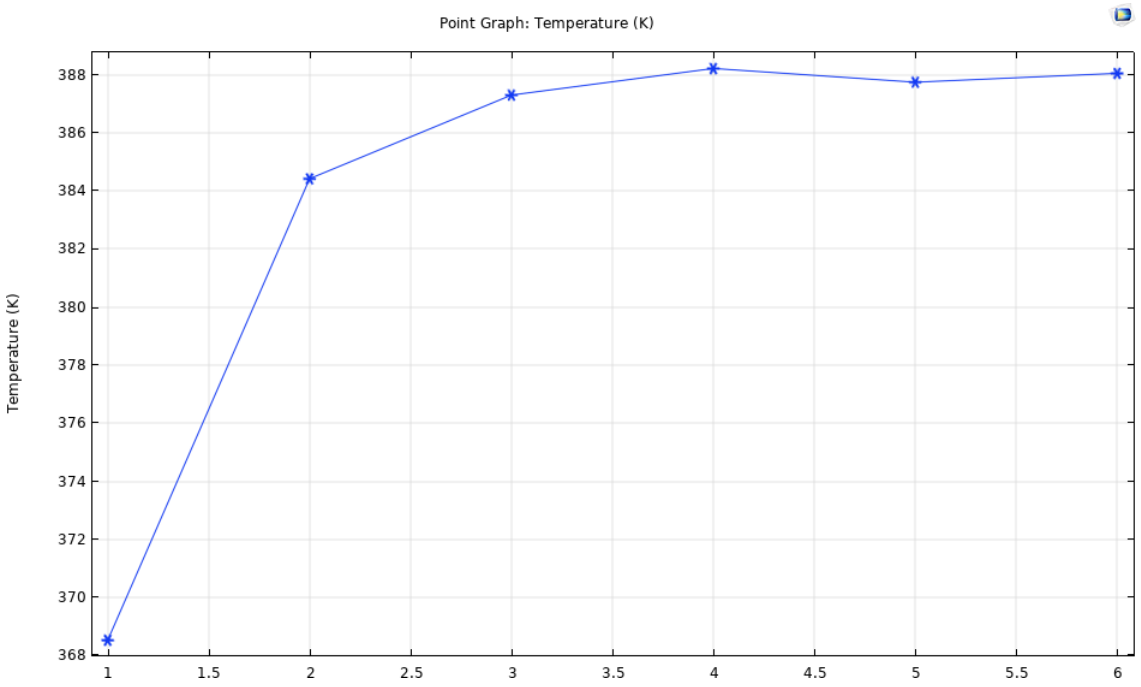

Figure 34. Results of the copper coil heating with the number of coils turns

This will significantly decrease the copper spiral heating. As the result, the distance between the power pulses can be much less. Therefore, the operating frequencies can be at least 10 times higher. It also should be noted that the distance between the sample and coils and the distance between two coils itself affects the magnetic field strength in the Ni-Mn-Ga sample significantly.

4.4 Study of the geometry of the single turn copper coil

One of the possible applications of the designed device is an MSM device which operates in a micro-scale. Such specific applications require quite small actuators and, hence, small coils to control them. For these purposes multi-turn coil is too complicated to produce.

For these purposes, it is required to decrease not only the inner radius of copper coils but also the modeled thickness of the MSM material, as the designed copper coils are significantly smaller than the distance between coils. Modeled distance between the coils is30 μm. This material thickness is usual for thin films that are achieved by an epitaxy process. These thin foils have a number of properties which cannot be observed in a bulk material. Such properties are explained by the increased role of the surface processes comparing to the bulk processes. Creation of these thin foils from

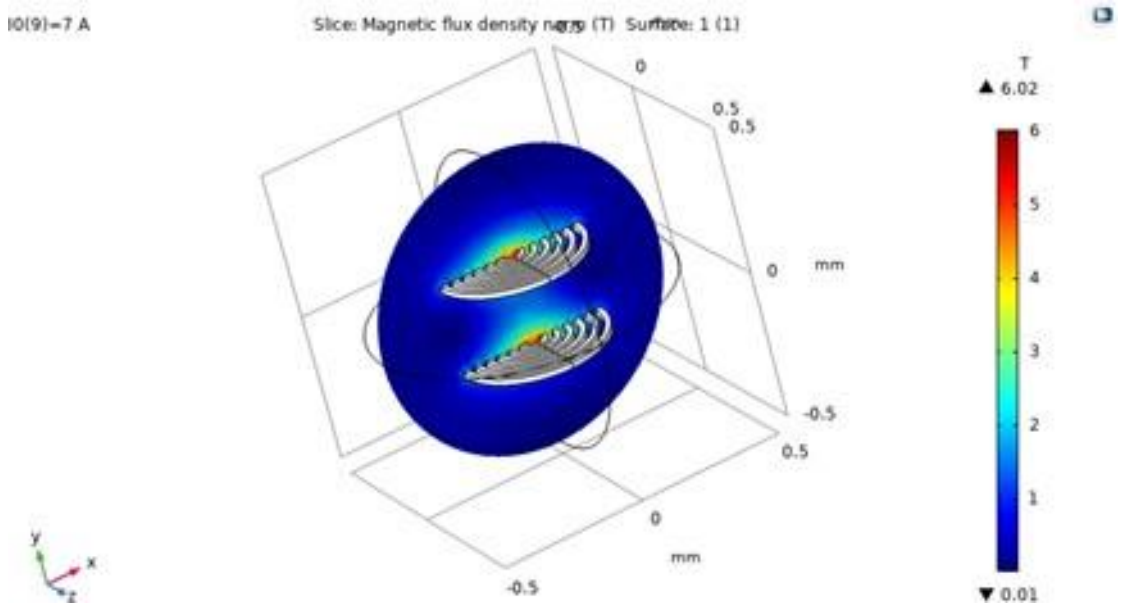

Figure 35. Modified geometry for magnetic field study (axonometric view)

Ni-Mn-Ga and studies of its new properties is a subject for a separate study.

The modeled magnetic field distribution is presented in the Fig. 41. As it can be seen from this figure, current system requires much less current for proper operation. This geometry can create a magnetic flux density of 0.3 T only with 0.2 A. Only 1 A is required to achieve the flux density of 0,61 T, which is more than the required value. The dependence of the magnetic flux density on current is presented in the Fig. 42.

Another positive side of this geometry is the less heating of the material. According to modeling (Fig. 43 and Fig. 44), it is possible to make the pulse length up to 2 ms, which is 10 times longer than the modeled pulse length for the experimental coil.

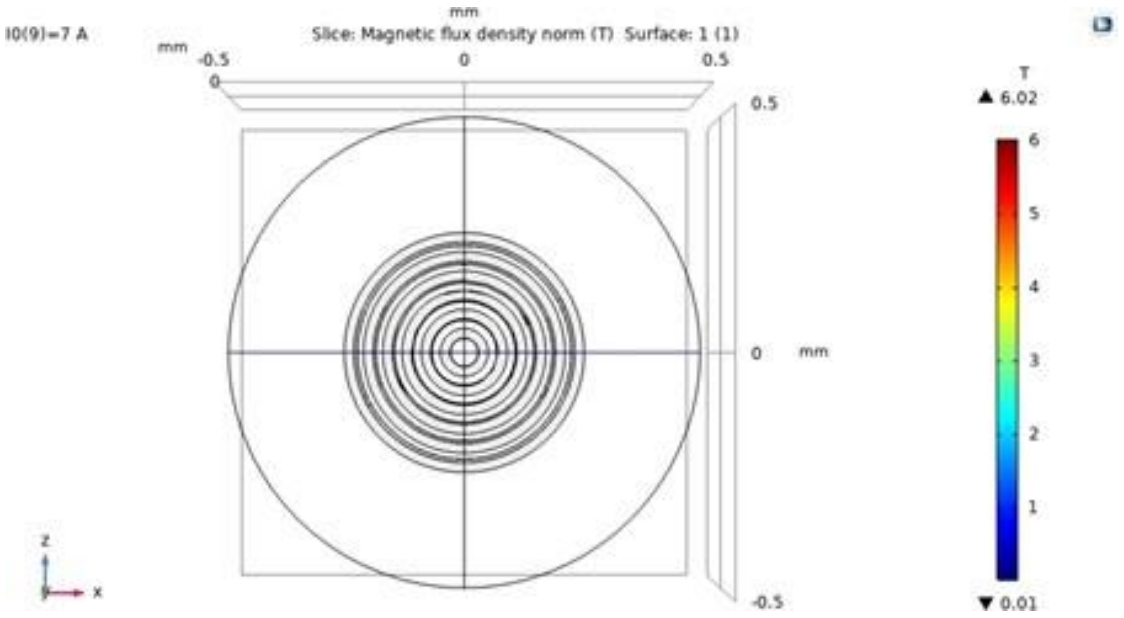

Figure 36. Modified geometry for magnetic field study (top view)

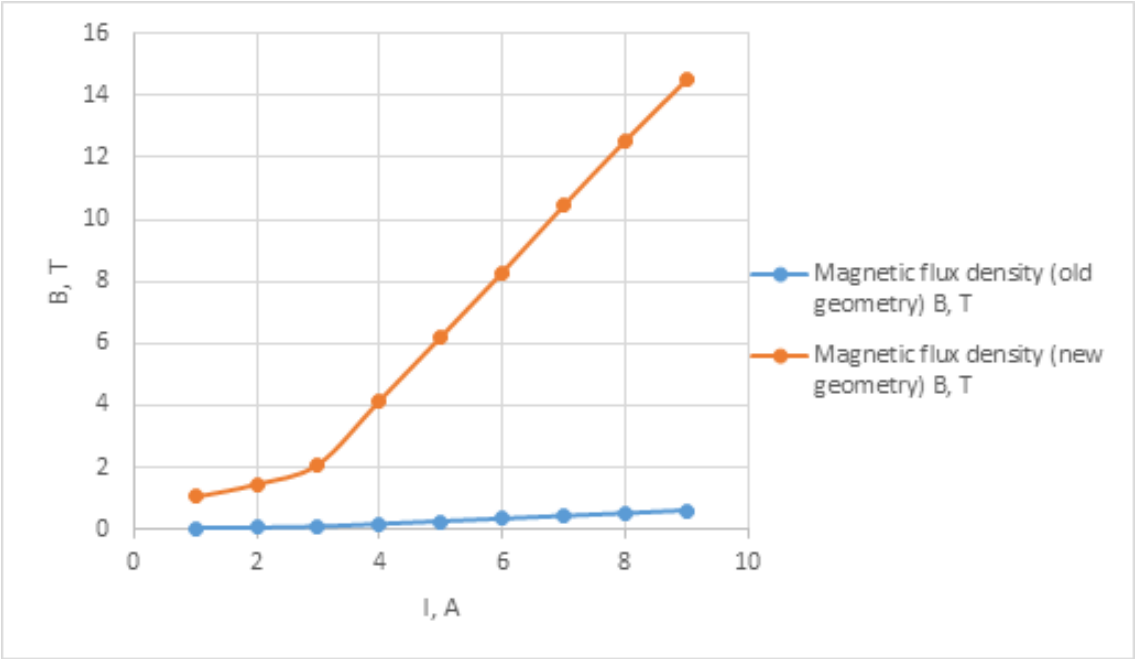

Figure 37. Magnetic flux density on current dependency

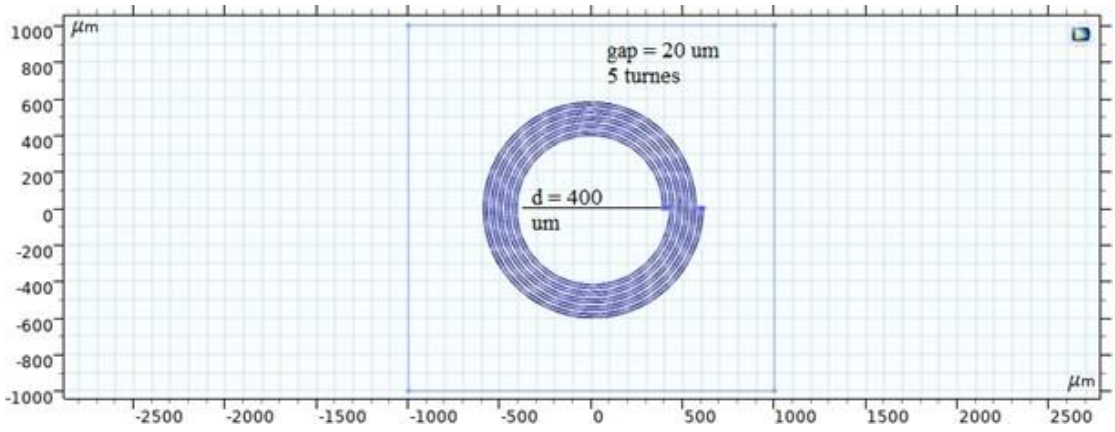

Figure 38. Model for heating properties estimation geometry

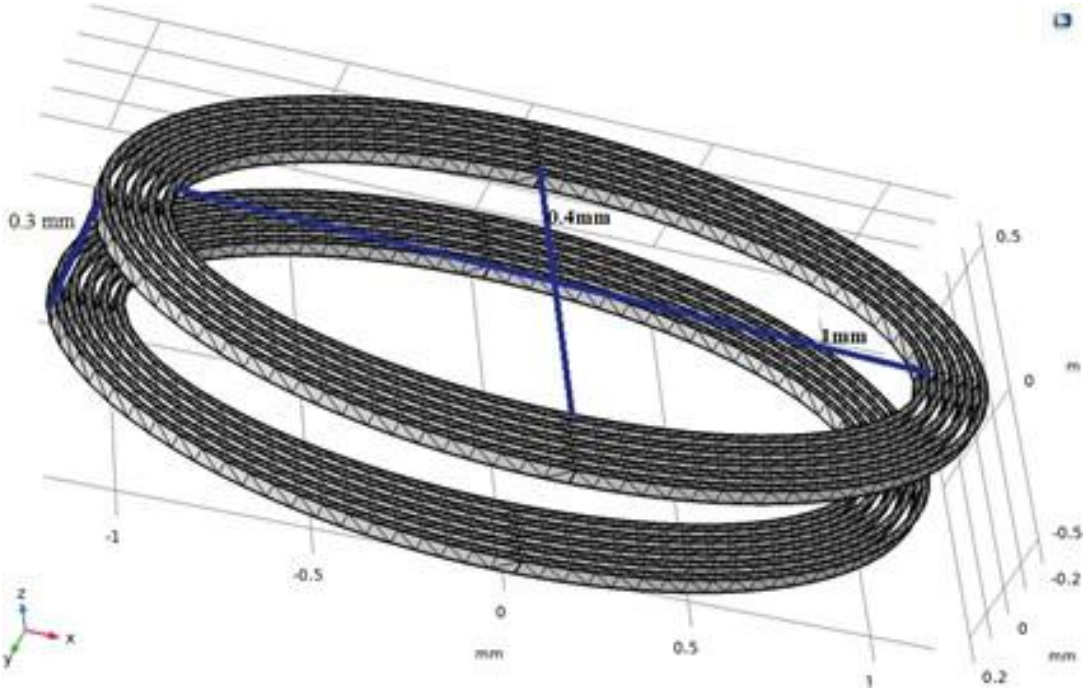

Figure 39. Rectangular sample model geometry

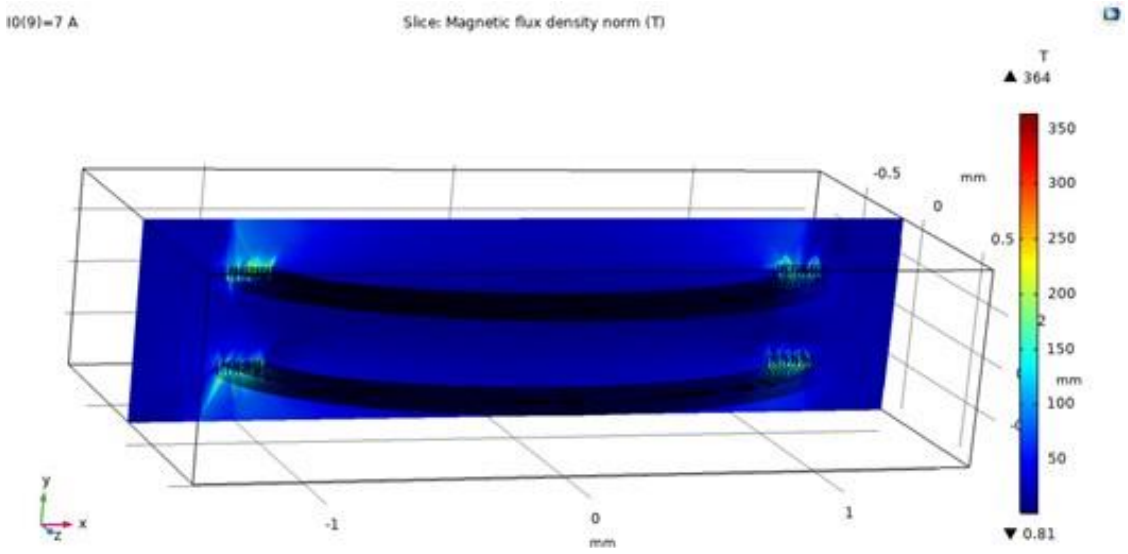

Figure 40. Rectangular sample modeling results

Table 6. Oval spiral modeling results.

Flux density B_{max}, T	Current I, A
2.48	0.5
2.48	0.7
2.69	1
3.04	2
3.29	3
3.44	4
3.87	5
3.92	6
4.19	7

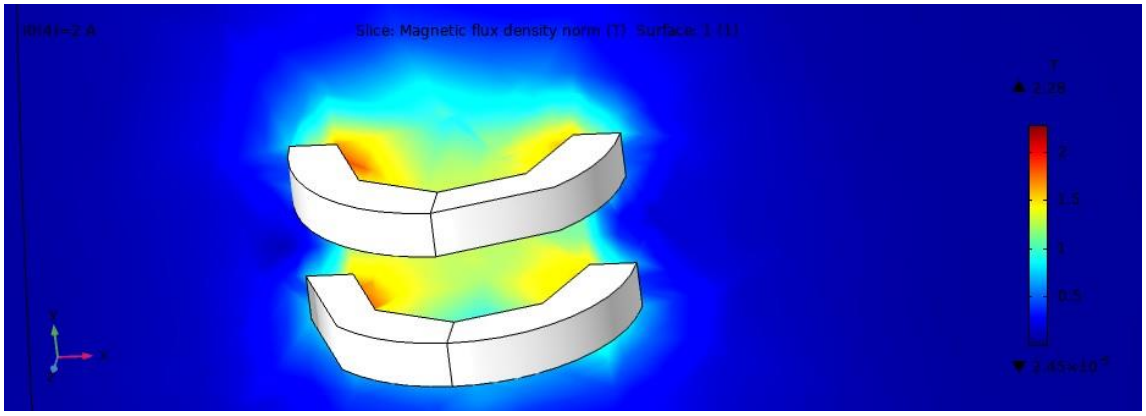

Figure 41. Modeled field distribution for single turn copper spiral

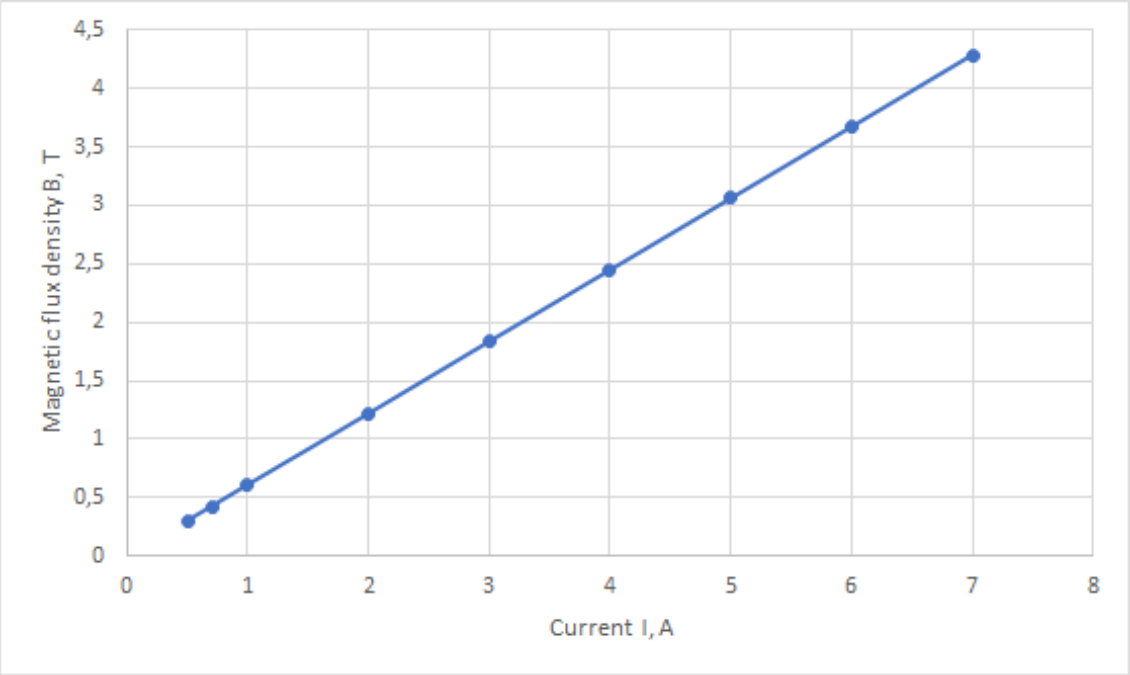

Figure 42. Modeled field distribution for single turn copper spiral

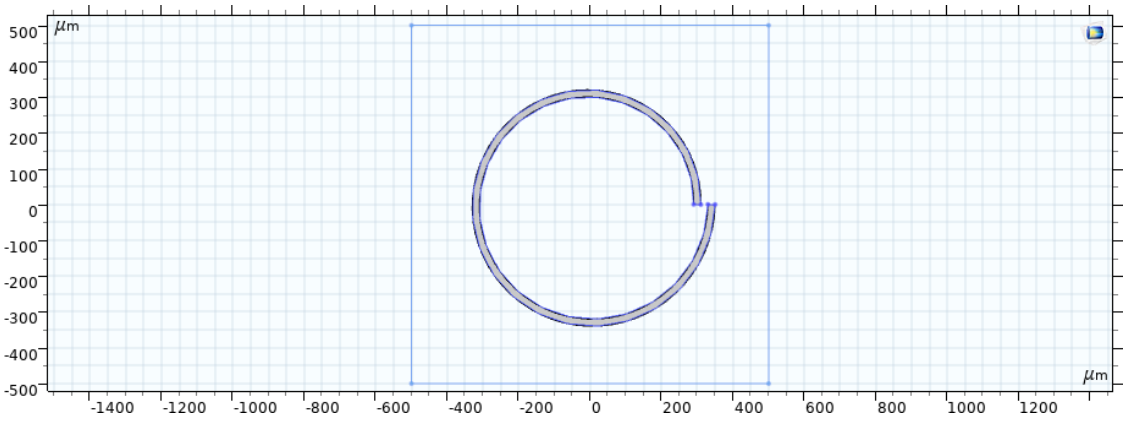

Figure 43. Modeled field distribution for single turn copper spiral

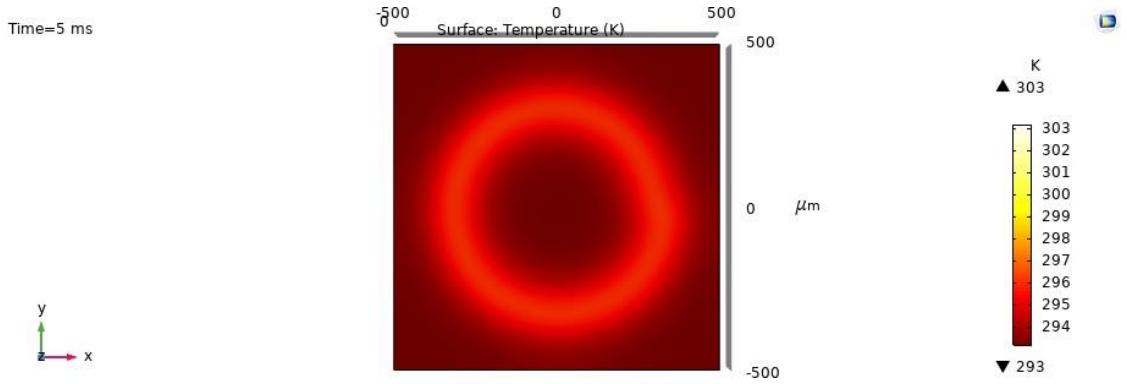

Figure 44. Modeled field distribution for single turn copper spiral

4 CONCLUSION

4.1 Current study

The received modeling results show that the magnetic flux density is highly dependent on the distance from coil to the place where the MSM sample is supposed to be placed. Therefore, it is required to recreate the geometry of the MSM sample.

Chapter 4 also contains the main dependencies for the designed copper coil input parameters. The main idea of the current geometry is to produce small enough coil to create the required magnetic field. The copper coil geometry can be changed with the width of the coil turn, gap between the turns, inner diameter, and number of turns. It is also worth remembering that all the observed parameters have a limited possibility for scaling down. Width of the conducting part and the gap between the turns are limited by the production capabilities. Moreover, all of the observed capabilities are modeled for spiral in the air. In other words, this part is not attached to the substrate. For quite high current that is passing through the coil, possibility of the short circuit increases.

Inner diameter in this system is limited by the dimensions of the MSM sample, as it supposed to be placed in the middle of the copper coil.

The last parameter, number of turns, is affectedby scaling down of the system less than the previous parameters. However, as it was described in the chapter 4, each new turn of the spiral makes less impact than the previous one.

It is also important to remember that this work is devoted to the system modeling. All the coil production process requires a separate study, which takes into account different production methods, such as pulsed laser ablation or lithography.

During this master thesis the copper coil geometry was designed. The geometry is de signed as an Archimedes' spiral.

4.2 Future work

The next step for studies of the MSM devices production is to create the way to scale down the coil to the modeled sizes. As it was shown in previous chapter, smaller dimensions decrease the minimum current that is required to create flux density B = 0.5 T. These adjustments will allow to decrease the energy that is spent on the magnetic field generation.

Also, it is required to make the model more accurate by adding the substrate both for the temperature and magnetic field modeling.

Further step in studies is to start testing an actual device prototypes. For these purposes, thin plate of Ni-Mn-Ga should be put in the middle of the working area of the coil. The prototypes can be studied as an electrical device. All the further studies for this type of the device are connected to the increase of the efficiency.

Another quite perspective research direction is the work with thin films of the MSM materials, as it was shown at the chapter 4. Lowering of the dimensions may significantly increase the control system efficiency.

REFERENCES

[1] Britannica, The Editors of Encyclopedia. "coil". Encyclopedia Britannica, 20 Jul. 1998. https://www.britannica.com/technology/coil, 2022. [Online; accessed April, 13, 2022].

[2] Elektromaker, what is an Inductor, 3 Sep. 2020. https://www.electromaker.io/blog/article/what-is-an-inductor, 2020. [Online; accessed April, 13, 2022].

[3] A. Sozinov, A.A. Likhachev, and K. Ullakko. Crystal structures and magnetic anisotropy properties of ni-mn-ga martensitic phases with giant magnetic-field-induced strain. *IEEE Transactions on Magnetics*, 38(5):2814–2816, 2002.

[4] Stephen A. Wilson, Renaud P.J. Jourdain, Qi Zhang, Robert A. Dorey, Chris R. Bowen, Magnus Willander, Qamar Ul Wahab, Magnus Willander, Safaa M. Al-hilli, Omer Nur, Eckhard Quandt, Christer Johansson, Emmanouel Pagounis, Manfred Kohl, Jovan Matovic, Björn Samel, Wouter van der Wijngaart, Edwin W.H. Jager, Daniel Carlsson, Zoran Djinovic, Michael Wegener, Carmen Moldovan, Rodica Iosub, Estefania Abad, Michael Wendlandt, Cristina Rusu, and Katrin Persson. New materials for micro-scale sensors and actuators: An engineering review. *Materials Science and Engineering: R: Reports*, 56(1):1–129, 2007.

[5] Uvanesh Kasiviswanathan, Chandan Kumar, Suruchi Poddar, Satyabrata Jit, Sanjeev Kumar Mahto, and Neeraj Sharma. Fabrication of msm-based biosensing device for assessing dynamic behavior of adherent mammalian cells. *IEEE Sensors Journal*, 20(17):9652–9659, 2020.

[6] Berta Spasova and Hans Gatzen. Simulation of an improved microactuator with discrete msm elements. *Materials Science Forum - MATER SCI FORUM*, 635:181–186, 12 2009.

[7] Krupa, M. M., Skirta, Y. B., Barandiaran, J.M., Ohtsuka, M., and Chernenko, V.A. Autonomous generator based on ni-mn-ga microactuator as a frequency selective element. *EPJ Web of Conferences*, 40:09001, 2013.

[8] J. M. Stephan, E. Pagounis, M. Laufenberg, P. Ruther, and O. Paul. Mechanical sensing based on ferromagnetic shape memory alloys. In *SENSORS, 2010 IEEE*, pages 2577–2580, 2010.

[9] Comsol Multiphysics official website, Comsol Multiphysics, Sweden. www.comsol.com, 2022. [Online; accessed February 16, 2022].

[10] Lasea modules official website, Datasheet for LS-Lab laser setup, Finland. https://www.lasea.eu/wp-content/uploads/2018/07/Datasheet-LS-Lab-1.pdf, 2022. [Online; accessed March 22, 2022].

[11] Kharanzhevsky E. and Krivilev M. *Physics of lasers, laser technologies and methods of mathematical modeling of laser action on matter. Tutorial.* Udmurt University Publishing House, 1st edition, 2011.

[12] L-C Xu and C.A. Siedlecki. 4.18 surface texturing and control of bacterial adhesion. In Paul Ducheyne, editor, *Comprehensive Biomaterials II*, pages 303–320. Elsevier, Oxford, 2017.